Supplementary material

Manifold lateralisation and variability in the language connectome at 7T

Lilit Dulyan[1-3*], Cesare Bortolami[4,5], Eva Guzmán Chacón[1], Ahmad Beyh[6], Michel Thiebaut de Schotten[3,7] & Stephanie J Forkel[1-3*]

Table 1. Descriptive statistics for lateralisation indices (LI) across seven language-recruited white matter tracts in a cohort of 164 participants. For each tract and diffusion metric, the table reports the mean, standard deviation, median, and results of the Shapiro–Wilk test for normality. A p-value < 0.05 indicates a significant deviation from a normal distribution (highlighted in grey).

Metric	Tract	Average	St. dev.	Median	Shape of data distribution	Shapiro–Wilk test p values
HMOA	AFl	-0.076	0.054	-0.073		0.145
Track count	AFl	-0.213	0.401	-0.191		p < 0.05
Voxel count	AFl	-0.139	0.252	-0.144		0.912
HMOA	AFa	0.1	0.081	0.111		p < 0.001
Track count	AFa	0.245	0.473	0.305		p < 0.001
Voxel count	AFa	0.322	0.346	0.37		p < 0.05
HMOA	AFp	-0.013	0.059	-0.013		0.093
Track count	AFp	-0.102	0.418	-0.083		0.29
Voxel count	AFp	-0.08	0.29	-0.071		0.08
HMOA	IFOF	-0.028	0.043	-0.023		0.198
Track count	IFOF	-0.001	0.361	-0.038		0.105
Voxel count	IFOF	-0.023	0.209	-0.028		0.552
HMOA	UF	0.071	0.095	0.058		p < 0.05
Track count	UF	0.318	0.375	0.383		p < 0.05
Voxel count	UF	0.323	0.298	0.348		0.502
HMOA	ILF	-0.033	0.063	-0.035		0.182
Track count	ILF	-0.277	0.359	-0.326		p < 0.05
Voxel count	ILF	-0.174	0.255	-0.193		0.162
HMOA	FAT	-0.022	0.048	-0.025		0.447
Track count	FAT	-0.548	0.338	-0.653	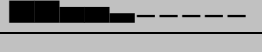	p < 0.001
Voxel count	FAT	-0.339	0.311	-0.34		p < 0.05

AFl: long segment of arcuate fasciculus, AFa: anterior segment of arcuate fasciculus, AFp: posterior segment of arcuate fasciculus, IFOF: inferior fronto-occipital fasciculus, UF: uncinate fasciculus, ILF: inferior longitudinal fasciculus, FAT: frontal aslant tract, HMOA: hindrance modulated orientational anisotropy.

Table 2. Descriptive statistics of raw diffusion metrics per hemisphere across seven language-recruited white matter tracts in 172 participants. For each tract, the table reports the percentage of participants with successful reconstruction, the average value, standard deviation, median, and the distribution shape of each metric. Metrics include hindrance modulated orientational anisotropy (HMOA), track count, and voxel count. The distribution icons provide a visual summary of the data spread across participants.

Side	Metric	Tract	Success of reconstruction	Average	St. dev.	Median	Distribution
Left	HMOA	AFl	99.42 %	0.026	0.003	0.026	
Right	HMOA	AFl	100 %	0.022	0.002	0.022	
Left	Track count	AFl	99.42 %	397.585	235.819	346	
Right	Track count	AFl	100 %	276.669	212.514	223.5	
Left	Voxel count	AFl	99.42 %	9848.561	2770.412	9923	
Right	Voxel count	AFl	100 %	7873.57	3559.552	7540.5	
Left	HMOA	AFa	98.84 %	0.02	0.004	0.02	
Right	HMOA	AFa	100 %	0.024	0.003	0.024	
Left	Track count	AFa	98.84 %	73.818	63.634	53.5	
Right	Track count	AFa	100 %	138.773	122.588	112	
Left	Voxel count	AFa	98.84 %	2164.418	1378.059	2008.5	
Right	Voxel count	AFa	100 %	4344.634	2217.278	4175.5	
Left	HMOA	AFp	100 %	0.019	0.002	0.019	
Right	HMOA	AFp	99.42 %	0.018	0.002	0.019	
Left	Track count	AFp	100 %	271.541	159.276	243	
Right	Track count	AFp	99.42 %	226.988	159.098	203	
Left	Voxel count	AFp	100 %	4098.233	1408.385	4219	
Right	Voxel count	AFp	99.42 %	3586.064	1506.497	3550	
Left	HMOA	IFOF	100 %	0.034	0.004	0.034	
Right	HMOA	IFOF	100 %	0.033	0.003	0.033	
Left	Track count	IFOF	100 %	160.378	101.262	137.5	
Right	Track count	IFOF	100 %	164.674	118.476	140	
Left	Voxel count	IFOF	100 %	8206.901	2713.365	8072	
Right	Voxel count	IFOF	100 %	7845.262	2627.782	7537.5	
Left	HMOA	UF	98.84 %	0.018	0.003	0.019	
Right	HMOA	UF	100 %	0.021	0.002	0.021	
Left	Track count	UF	98.84 %	24.665	20.114	19	
Right	Track count	UF	100 %	50.384	35.474	40	
Left	Voxel count	UF	98.84 %	1316.471	847.955	1255	
Right	Track count	UF	100 %	2588.797	1341.312	2412.5	
Left	HMOA	ILF	100 %	0.03	0.004	0.029	
Right	HMOA	ILF	100 %	0.028	0.003	0.027	
Left	Track count	ILF	100 %	121.401	81.057	101	
Right	Track count	ILF	100 %	62.895	43.576	53	
Left	Track count	ILF	100 %	5738.797	2276.582	5590	
Right	Voxel count	ILF	100 %	3996.89	1765.773	3823.5	
Left	HMOA	FAT	100 %	0.014	0.001	0.014	
Right	HMOA	FAT	98.26 %	0.014	0.001	0.013	
Left	Track count	FAT	100 %	369.849	316.706	275.5	
Right	Track count	FAT	98.26 %	84.923	71.723	64	
Left	Voxel count	FAT	100 %	4290.326	2191.34	3964	
Right	Voxel count	FAT	98.26 %	2171.391	1418.526	1996	

AFl: long segment of arcuate fasciculus, AFa: anterior segment of arcuate fasciculus, AFp: posterior segment of arcuate fasciculus, IFOF: inferior fronto-occipital fasciculus, UF: uncinate fasciculus, ILF: inferior longitudinal fasciculus, FAT: frontal aslant tract, HMOA: hindrance modulated orientational anisotropy.

Table 3. Results of the permutation analysis assessing interhemispheric variability (Variability Index, VI) across seven language-recruited tracts and three white matter metrics: hindrance modulated orientational anisotropy (HMOA), track count, and voxel count. The VI index reflects the relative variability between hemispheres, with negative values indicating greater variability in the left hemisphere and positive values indicating greater variability in the right hemisphere. P-values are derived from 100,000 permutations testing the null hypothesis of equal interhemispheric variability. Statistically significant results after Bonferroni correction (adjusted alpha = 0.0021 for 24 comparisons).

Metric	Tract	VI index	p-value
HMOA	AFl	-0.14508208	0.01185
Track count	AFl	0.01431493	0.81293
Voxel count	AFl	0.14789377	0.03171
HMOA	AFa	0.08651476	0.17211
Track count	AFa	0.28431373	0.00025
Voxel count	AFa	0.23738090	0.00021
HMOA	AFp	0.02728348	0.66204
Track count	AFp	-0.11568123	0.08820
Voxel count	AFp	0.04563691	0.50930
HMOA	IFOF	-0.12637746	0.02884
Track count	IFOF	-0.08225108	0.24972
Voxel count	IFOF	-0.05419510	0.36589
HMOA	UF	-0.20324855	0.00963
Track count	UF	0.30303030	0.00003
Voxel count	UF	0.31873654	0.00002
HMOA	ILF	0.11786570	0.03962
Track count	ILF	-0.32867133	0.00000
Voxel count	ILF	-0.18732933	0.00072
HMOA	FAT	0.05843268	0.29175
Track count	FAT	-0.58252427	0.00000
Voxel count	FAT	-0.18649391	0.00361
HMOA	Average	-0.14200009	0.01783
Track count	Average	-0.12035398	0.03160
Voxel count	Average	0.02747854	0.65717

AFl: long segment of arcuate fasciculus, AFa: anterior segment of arcuate fasciculus, AFp: posterior segment of arcuate fasciculus, IFOF: inferior fronto-occipital fasciculus, UF: uncinate fasciculus, ILF: inferior longitudinal fasciculus, FAT: frontal aslant tract, HMOA: hindrance modulated orientational anisotropy, VI: variability index.

Table 4. Posterior summary of the full Bayesian regression model predicting **Language processing (accuracy)** performance from lateralisation indices of language-recruited white matter tracts. Estimates (posterior means), standard errors, and 95% credible intervals for all regression coefficients are reported. Across all predictors, credible intervals included zero, indicating no robust evidence for an association between LI and behavioural performance.

Predictor	**Estimate**	**Est.Error**	**l-95% CI**	**u-95% CI**	**Rhat**	**Bulk_ESS**	**Tail_ESS**
Intercept	95,35598	0,765659	93,80979	96,77632	1,000132	4880,633	3238,409
HMOA_AFl	-0,01056	0,481795	-0,8973	0,890509	1,002759	4519,732	2087,69
TC_AFl	0,059065	0,471398	-0,85539	0,902664	1,002386	5124,381	1963,302
VC_AFl	0,042845	0,483452	-0,90002	0,92798	1,002277	4124,873	1925,155
HMOA_AFa	-0,00898	0,496463	-0,91744	0,909615	1,000639	5466,819	2465,611
TC_AFa	-0,10828	0,459751	-0,91552	0,814774	1,001022	3811,463	2048,844
VC_AFa	0,039786	0,487319	-0,87256	0,916552	1,000025	4817,323	2277,41
HMOA_AFp	0,015211	0,506656	-0,91886	0,929689	1,000337	4370,669	1797,927
TC_AFp	0,167877	0,45593	-0,78263	0,934105	1,001245	4943,78	2376,495
VC_AFp	0,082838	0,48499	-0,84866	0,912687	1,00193	4752,788	2560,529
HMOA_IFOF	-0,00231	0,481279	-0,88646	0,900608	1,002778	4659,314	2212,385
TC_IFOF	-0,06211	0,46104	-0,91104	0,843658	1,001384	4361,377	2332,222
VC_IFOF	-0,03129	0,47276	-0,89384	0,873532	1,000166	4832,534	2295,473
HMOA_UF	-0,05418	0,492779	-0,93115	0,889765	1,002169	5023,9	1947,221
TC_UF	-0,214	0,472488	-0,95723	0,817714	1,00041	4593,738	2248,57
VC_UF	-0,1665	0,468943	-0,93816	0,808424	0,999772	4914,715	1794,754
HMOA_ILF	0,018226	0,487928	-0,88878	0,904851	1,002167	4802,355	2279,01
TC_ILF	0,08632	0,476615	-0,8563	0,927953	1,002633	4764,321	1813,527
VC_ILF	0,08246	0,48217	-0,86351	0,927329	1,000576	4687,92	2016,177
HMOA_FAT	0,024162	0,481368	-0,88219	0,907041	1,003226	4458,484	2031,507
TC_FAT	0,0397	0,48963	-0,87617	0,910581	1,002534	4804,302	2437,185
VC_FAT	0,036547	0,48294	-0,89869	0,914476	1,002675	5159,262	2069,985

Table 5. Posterior summary of the full Bayesian regression model predicting **Language processing (reaction time)** performance from lateralisation indices of language-recruited white matter tracts. Estimates (posterior means), standard errors, and 95% credible intervals for all regression coefficients are reported. Across all predictors, credible intervals included zero, indicating no robust evidence for an association between LI and behavioural performance.

Predictor	**Estimate**	**Est.Error**	**l-95% CI**	**u-95% CI**	**Rhat**	**Bulk_ESS**	**Tail_ESS**
Intercept	3290,664	24,69292	3241,456	3338,821	0,99993	5026,528	3075,689
HMOA_AFl	0,00119	0,493601	-0,91429	0,908792	1,006454	4443,435	2081,961
TC_AFl	-0,01046	0,490698	-0,90309	0,888323	1,002446	5000,665	2271,569
VC_AFl	-0,0101	0,497361	-0,90301	0,903327	1,002137	4707,21	2218,235
HMOA_AFa	-0,01501	0,485835	-0,9081	0,909483	1,008981	4361,091	2052,574
TC_AFa	-0,01391	0,494781	-0,91815	0,88752	1,002053	3974,705	1472,187
VC_AFa	0,008793	0,488547	-0,89828	0,901689	1,001542	4318,198	1754,884
HMOA_AFp	0,000348	0,503416	-0,89601	0,90602	1,002961	4649,254	2444,642
TC_AFp	-0,01005	0,490266	-0,90176	0,89477	1,002812	4236,205	1994,223
VC_AFp	0,002968	0,495769	-0,90896	0,892875	1,000703	5516,933	2396,409
HMOA_IFOF	0,007671	0,494077	-0,89263	0,907449	1,000726	5152,173	2054,737
TC_IFOF	0,011859	0,485085	-0,89414	0,911319	1,002551	4386,468	2120,977
VC_IFOF	-0,01359	0,496495	-0,92231	0,90384	1,001148	4891,812	2299,503
HMOA_UF	-0,00461	0,487964	-0,90055	0,909484	1,00014	5264,599	2581,415
TC_UF	0,005827	0,493892	-0,91079	0,914413	1,00155	4192,263	1901,527
VC_UF	0,003635	0,497278	-0,89783	0,913505	1,000298	6257,65	2164,5
HMOA_ILF	-0,00191	0,506233	-0,92372	0,906891	0,999797	5480,001	2284,58
TC_ILF	-0,0011	0,498393	-0,92083	0,92012	1,001176	5067,683	1801,308
VC_ILF	-7,3E-06	0,494846	-0,901	0,909526	1,000454	4573,417	2190,553
HMOA_FAT	-0,01354	0,483334	-0,91426	0,896027	1,00016	4857,554	2337,445
TC_FAT	-0,01551	0,48617	-0,89976	0,885531	1,002534	4892,023	2195,1
VC_FAT	-0,00178	0,493818	-0,90873	0,910258	1,002726	4717,524	2070,048

Table 6. Posterior summary of the full Bayesian regression model predicting **Tone Discrimination (accuracy)** performance from lateralisation indices of language-recruited white matter tracts. Estimates (posterior means), standard errors, and 95% credible intervals for all regression coefficients are reported. Across all predictors, credible intervals included zero, indicating no robust evidence for an association between LI and behavioural performance.

Predictor	**Estimate**	**Est.Error**	**l-95% CI**	**u-95% CI**	**Rhat**	**Bulk_ESS**	**Tail_ESS**
Intercept	4,296479	0,245893	3,82123	4,783916	1,000533	5064,078	3627,482
HMOA_AFl	-0,0096	0,482431	-0,89187	0,893649	1,002343	3942,28	1888,764
TC_AFl	0,039448	0,309689	-0,57235	0,649271	1,002463	4481,556	2497,359
VC_AFl	-0,09582	0,420711	-0,89766	0,747266	1,000748	4019,784	2109,057
HMOA_AFa	-0,11037	0,455115	-0,91887	0,836098	1,002306	5509,739	2120,643
TC_AFa	-0,17384	0,306727	-0,78598	0,423898	1,001315	4136,466	2025,75
VC_AFa	-0,04023	0,395187	-0,8181	0,75841	1,001918	4615,385	2388,972
HMOA_AFp	0,011344	0,479112	-0,89855	0,898257	1,001216	5813,803	2361,902
TC_AFp	0,087698	0,322534	-0,54812	0,715331	1,003714	4441,474	2402,965
VC_AFp	-0,06995	0,416711	-0,85749	0,7707	1,002149	3699,857	2508,989
HMOA_IFOF	0,098159	0,481544	-0,85706	0,93787	1,002796	5620,739	2179,554
TC_IFOF	0,446816	0,304315	-0,17269	0,961007	1,000461	3899,554	1823,185
VC_IFOF	-0,19208	0,440301	-0,92966	0,718696	1,000127	4407,178	2343,755
HMOA_UF	-0,18701	0,456404	-0,93824	0,754389	1,00391	5739,552	2018,031
TC_UF	0,320315	0,342011	-0,37838	0,932116	0,999984	4429,005	2316,12
VC_UF	0,039378	0,407834	-0,76679	0,839527	1,000254	4655,358	2438,218
HMOA_ILF	-0,04076	0,454232	-0,88408	0,856582	1,001559	7067,636	1851,239
TC_ILF	0,182707	0,329383	-0,46479	0,815662	1,000957	3899,248	2262,565
VC_ILF	-0,33824	0,394476	-0,95893	0,51969	1,000081	3509,081	2091,493
HMOA_FAT	-0,10338	0,480911	-0,92885	0,839009	1,002083	6877,668	2527,767
TC_FAT	0,02883	0,378085	-0,72004	0,781092	1,002283	4126,923	2453,87
VC_FAT	-0,1192	0,397688	-0,86136	0,678335	1,001479	3884,132	2350,492

Table 7. Posterior summary of the full Bayesian regression model predicting **Picture Vocabulary (accuracy)** performance from lateralisation indices of language-recruited white matter tracts. Estimates (posterior means), standard errors, and 95% credible intervals for all regression coefficients are reported. Across all predictors, credible intervals included zero, indicating no robust evidence for an association between LI and behavioural performance.

Predictor	**Estimate**	**Est.Error**	**l-95% CI**	**u-95% CI**	**Rhat**	**Bulk_ESS**	**Tail_ESS**
Intercept	111,1299	1,253424	108,6566	113,52	1,001036	5958,109	3050,404
HMOA_AFl	-0,02543	0,490803	-0,91499	0,911818	1,000644	4920,179	1780,764
TC_AFl	-0,01837	0,472252	-0,88913	0,879818	1,001557	5563,703	2254,862
VC_AFl	-0,03145	0,480924	-0,91151	0,859301	1,001235	4476,367	2071,544
HMOA_AFa	-0,0257	0,501107	-0,91786	0,916254	1,001816	5028,457	2190,893
TC_AFa	-0,07488	0,480077	-0,91826	0,845435	1,001233	5640,652	2395,696
VC_AFa	-0,06371	0,487044	-0,91355	0,870929	1,002731	4936,93	2316,015
HMOA_AFp	-0,01151	0,481945	-0,88476	0,879374	1,001433	6185,793	2629,998
TC_AFp	0,003365	0,489353	-0,90035	0,907361	1,003928	5831,021	1974,792
VC_AFp	0,019721	0,479493	-0,86784	0,901215	1,003621	5193,596	2313,132
HMOA_IFOF	0,002092	0,492338	-0,88965	0,901518	1,002549	5928,938	2033,152
TC_IFOF	-0,14199	0,477003	-0,94854	0,852974	1,002729	3976,405	1644,85
VC_IFOF	-0,05087	0,498556	-0,92092	0,891168	1,000432	5008,234	2332,292
HMOA_UF	0,008311	0,503691	-0,93445	0,921176	1,000655	5376,143	1851,627
TC_UF	-0,05935	0,489561	-0,93222	0,880998	1,002532	4202,872	1656,351
VC_UF	-0,02004	0,499663	-0,93528	0,913516	1,002726	5284,11	1839,423
HMOA_ILF	0,003422	0,498661	-0,91246	0,907055	1,005384	4551,16	2055,774
TC_ILF	-0,01598	0,480735	-0,8936	0,86755	1,002022	5334,882	2153
VC_ILF	0,040663	0,480333	-0,87748	0,915317	1,003533	5381,233	1708,163
HMOA_FAT	0,001165	0,484205	-0,89305	0,909276	1,000477	5248,524	1903,214
TC_FAT	0,162135	0,481878	-0,81487	0,946656	1,000121	4675,029	2095,35
VC_FAT	0,12868	0,469549	-0,8292	0,932339	1,001812	5398,018	1934,658

Table 8. Posterior summary of the full Bayesian regression model predicting **Oral Reading Recognition (accuracy)** performance from lateralisation indices of language-recruited white matter tracts. Estimates (posterior means), standard errors, and 95% credible intervals for all regression coefficients are reported. Across all predictors, credible intervals included zero, indicating no robust evidence for an association between LI and behavioural performance.

Predictor	**Estimate**	**Est.Error**	**l-95% CI**	**u-95% CI**	**Rhat**	**Bulk_ESS**	**Tail_ESS**
Intercept	109,0505	1,237996	106,6934	111,5358	1,000845	5521,775	3223,118
HMOA_AFl	-0,01829	0,495369	-0,9194	0,907201	1,000764	4300,915	2284,135
TC_AFl	-0,03476	0,484525	-0,91235	0,872736	1,000637	4530,323	2431,323
VC_AFl	-0,01548	0,489701	-0,91562	0,891505	1,00082	5024,3	1813,039
HMOA_AFa	-0,01015	0,492217	-0,90892	0,910107	1,004078	4550,412	1997,102
TC_AFa	-0,04031	0,4922	-0,92641	0,882705	1,001591	4583,884	2025,192
VC_AFa	-0,01343	0,490289	-0,90102	0,877234	1,003197	4894,698	1953,599
HMOA_AFp	-0,02286	0,504539	-0,93199	0,922776	1,001853	5106,657	1981,554
TC_AFp	-0,01078	0,492643	-0,90565	0,909119	1,00332	5022,461	2246,532
VC_AFp	-0,00618	0,480756	-0,87545	0,896345	1,000488	5299,607	2516,34
HMOA_IFOF	-0,00063	0,49102	-0,89183	0,891816	1,000816	5252,198	2188,397
TC_IFOF	-0,14297	0,474788	-0,94473	0,840814	1,003247	4228,651	1975,805
VC_IFOF	-0,01135	0,49308	-0,91961	0,902309	1,001308	5066,756	2086,482
HMOA_UF	0,022871	0,487513	-0,87621	0,898946	1,002312	4575,201	2261,485
TC_UF	0,012377	0,489487	-0,88837	0,908249	1,000961	4935,754	2083,24
VC_UF	0,046826	0,490391	-0,88663	0,925525	1,002622	4798,455	2212,944
HMOA_ILF	0,017432	0,487944	-0,88532	0,916234	1,002966	4560,197	2191,741
TC_ILF	0,034648	0,482991	-0,8762	0,91819	1,000806	5395,864	2094,446
VC_ILF	0,033568	0,493291	-0,86918	0,906646	1,000664	5439,386	2584,283
HMOA_FAT	-0,00776	0,478527	-0,89583	0,882678	1,001972	5371,321	2212,164
TC_FAT	0,132457	0,471982	-0,80457	0,925407	1,002585	4986,839	2341,518
VC_FAT	0,115546	0,487156	-0,85634	0,937742	1,000282	4804,649	2066,414

Table 9. Overview of Common Diffusion-Based White Matter Atlases. This table summarises key characteristics of white matter atlases based on diffusion tractography. Each atlas is evaluated for its inclusion of major tract classes—association fibres, commissural fibres, projection fibres, U-fibres, and cerebellar fibres—as well as sample size and demographics. We indicate the tractography algorithm used (e.g. tensor-based, UKF, CSD) and whether key language-recruited tracts are included or missing, with tract definitions based on commonly accepted anatomical conventions. The final column notes whether the tract dissection was performed manually, automatically, or through a hybrid approach. Tract abbreviations: AFl = long segment of arcuate fasciculus, AFa = anterior segment, AFp = posterior segment, IFOF = inferior fronto-occipital fasciculus, ILF = inferior longitudinal fasciculus, UF = uncinate fasciculus, FAT = frontal aslant tract, tSLF = superior longitudinal fasciculus - temporal branch. Algorithm abbreviations: T-B = tensor-based, SD = spherical deconvolution, CSD = constrained spherical deconvolution, MSMT-CSD = multi-shell multi-tissue CSD, MSCM-SD = multi-shell compartment spherical deconvolution, UKF = Unscented Kalman Filter, AFQ = Automated Fibre Quantification, QBI = Q-ball imaging, QSDR = Q-space diffeomorphic reconstruction. Dataset abbreviations: HCP = Human Connectome Project, BLSA = Baltimore Longitudinal Study of Aging, VU = Vanderbilt University, CHCP = Chinese Connectome Project. N.R.: not reported, N.p.: number of participants.

Atlas	N Asso. fibers	N Com. fibres	N Proj. fibers	N U-fibers	N Cereb. fibers	N p.	Demographics Mean age, SD, sex	Algorithm	Language - recruited tracts included	Language - recruited tracts missing	Dissection method
Catani et al. 2002	6	2	2	0	0	1	39 y.o. male	T-B	AFl/SLF, ILF, UF, IFOF	AFa, AFp, FAT	manual
Catani and Thiebaut de Schotten 2008	5	2	2	0	3	12	NR, 34.3 ± 5.7, 100% M.	T-B	AFl, ILF, UF, IFOF	AFa, AFp, FAT	manual
Hua et al. 2008	7	2	2	0	0	28	NR, 29 ± 7.9; 39% F.	T-B	tSLF, ILF, UF, IFOF	AFl, AFa, AFp, FAT	manual
Mori et al. 2008	11	3	12	0	3	81	18–59, 38.63±NR; 48 % F.	T-B	ILF, UF, IFOF	AFl, AFa, AFp, FAT	manual
Rojkova et al. 2016	13	3	5	15	0	57	22-71, 45.45 ±14.79, 50% F.	SD	AFl, AFa, AFp, ILF, UF, IFOF, FAT		manual
Wakana et al. 2007	7	2	2	0	0	10	NR, 26.1± 5.48, 50% F.	T-B	ILF, UF, IFOF	AFL, AFa, AFp, FAT	manual
Maffei et al. 2021	10	9	6	0	1	16	NR, HCP	CSD & MSMT-CSD	AFl, UF, ILF, FAT	AFa, AFp, IFOF	manual
Radwan et al. 2022	15	8	12	0	3	20	22-35, NR, 50% F.	MSMT-CSD	AFl, ILF, UF, IFOF, FAT	AFa, AFp	hybrid
Li et al. 2024	11	7	10	8	6	306	22-37, 24.2 ± 1.4, 47% F. (west, n=153, HCP); 22-37, 23.9 ± 2.4; 44% F. (east, n=153, CHCP)	UKF	AFl, ILF, UF, IFOF	AFa, AFp, FAT	hybrid
Zhang et al. 2018	12	7	9	8	5	100	22–36, 29.1±3.7, 54% F.	UKF	AFl, ILF, UF, IFOF	AFa, AFp, FAT	hybrid
Mori et al. 2005	5	1	9	0	3	1	NR	T-B	ILF, UF, IFOF	AFl, AFa, AFp, FAT	manual
Hansen et al. 2021	7	2	2	0	0	2326	22-35, 28.8 ± 3.5, 54% F. (HCP); 22.4-95.1,66.2 ±	T-B; AFQ & AFQ-clipped	AFl, ILF, UF, IFOF	AFa, AFp, FAT	automatic

	7	2	10	0	3		14.82, 55% F. (BLSA); 18-75, 29.7 ± 11.5, 56% F. (VU)	SD; Recobundles	AFl, ILF, IFOF, UF, FAT	AFa, AFp,	
	9	9	20	0	3			CSD; TractSeg	AFl, ILF, UF, IFOF	AFa, AFp, FAT	
	6	2	2	0	0			Ball-and-stick; Tracula	ILF, UF	AFl, AFa, AFp, IFOF, FAT	
	12	3	7	0	1			Ball-and-stick; Xtract	AFl, ILF, UF, IFOF, FAT	AFa, AFp	
Hagler et al. 2009	7	3	3	0	0	21	21–52, 33 ± 10.2, 52% F.	T-B	tSLF, ILF, UF, IFOF	AFl, AFa, AFp, FAT	manual
Yendiki et al. 2011	6	2	2	0	0	33	NR, 42±10, 42% F.	T-B	tSLF, ILF, UF	AFl, AFa, AFp, IFOF, FAT	manual
Suarez et al. 2012	2	1	3	0	0	20	NR, 17.8 ±1.1, 50% F.	T-B	-	AFl, AFa, AFp, ILF, IFOF, UF, FAT	manual
Ros et al. 2013	5	2	2	0	0	15	NR	T-B	tSLF, ILF, IFOF, UF	AFl, AFa, AFp, FAT	hybrid
van Baarsen et al. 2016	0	0	0	0	3	90	22-35, 30, 61% F.	Ball-and-Stick model	-	AFl, AFa, AFp, ILF, IFOF, UF, FAT	hybrid
Tang et al. 2018	0	0	6	0	6	20	NR, 50% (HCP)	MSCM-SD	-	AFl, AFa, AFp, ILF, IFOF, UF, FAT	manual
Guevara et al. 2012	9	4	6	47 (left) 47(symmetrised right)	0	12	NR, adults	SD	AFl, AFa, AFp, ILF, IFOF, UF	FAT	hybrid

Guevara et al. 2017	0	0	0	50	0	79	NR; 23.6±5.2; 39% F.	QBI	-	AFl, AFa, AFp, ILF, IFOF, UF, FAT	automatic
Román et al. 2017	0	0	0	44 (left) 49 (right)	0	74	NR, 23.6 ± 5.2; 42% F.	QBI	-	AFl, AFa, AFp, ILF, IFOF, UF, FAT	automatic
Román et al. 2022	0	0	0	267 (left); 258 (right)	0	100	NR (HCP)	CSD	-	AFl, AFa, AFp, ILF, IFOF, UF, FAT	automatic
O'Donnell and Westin 2007	5	1	2	0	2	10	NR	T-B	AFl, ILF, IFOF, UF	AFa, AFp, FAT	hybrid
Yeh et al. 2018	10	3	17+5 cranial nerves	1 (combined)	5	842	22-36, NR, 56% F. (HCP)	QSDR	AFl, ILF, IFOF, UF, FAT	AFa, AFp	hybrid
Yoo et al. 2015	5	0	2	0	0	12	21-40, 32.8±5.5, 100% M	QBI	ILF, IFOF, UF	AFl, AFa, AFp, FAT	hybrid
O'Donnell et al. 2017	4	0	1	0	0	10	NR (HCP)	UKF	AFl, ILF, IFOF, UF	AFl, AFa, AFp, FAT	hybrid
Thiebaut de Schotten et al. 2011	7	2	6	3	0	40	18-22, NR, 50% fem.	T-B	AFl, AFa, AFp ILF, IFOF, UF	FAT	manual

Table 10. This table provides an overview of published and unpublished studies reporting hemispheric asymmetries in white matter tracts commonly associated with language. Reported measures include HMOA (Hindrance Modulated Orientational Anisotropy), tract volume, number of streamlines, and fractional anisotropy (FA). Each entry specifies the tractography method used, sample size (N), demographic details (age, sex), statistical test employed, and success rate of reconstruction of white matter tract in the left and right hemisphere in %. AFl: long segment of arcuate fasciculus, AFa: anterior segment of arcuate fasciculus, AFp: posterior segment of arcuate fasciculus, IFOF: inferior fronto-occipital fasciculus, UF: uncinate fasciculus, ILF: inferior longitudinal fasciculus, FAT: frontal aslant tract, HMOA: hindrance modulated orientational anisotropy, SR: Success rate, NR: not reported, N: sample size; #: The information was extracted based on the reported data; Algorithm abbreviations: T-B = tensor-based, SD = spherical deconvolution, CSD = constrained spherical deconvolution, GQI = Generalized Q-Sampling Imaging

	Study	HMOA	Volume	Streamlines	FA	Algorithm	N	Demogr.	Stat.Test	SR (left,%)	SR (right,%)
FAT	Catani et al. 2012	-	left	-	-	SD	13	NR	unpaired t-test	NR	NR
	Briggs et al. 2019	-	bilateral	-	-	GQI	10	23-34, 29.4±3.9, 60% F. #	unpaired t-test	NR	NR
	Guzman et al, unpublished	left	bilateral	bilateral	bilateral	SD	198	18-30, 23±3, 73% F.	one-sample t-test	100%	100%
	Rojkova et al. 2016	bilateral#	bilateral#	-	right#	SD	57	22-71, 45.45 ±14.79, 50% F.	summary stats based on unpaired t-test	100%	100%
	This study	left	left	left	-	SD	172	22-36, 29.3±3.3, 61% F.	one-sample t-test	100%	98,26%
IFOF	Briggs et al. 2019	-	bilateral	-	-	GQI	10	23-34, 29.4±3.9, 60% F. #	unpaired t-test	NR	NR
	Forkel et al. 2014	-	bilateral	-	-	SD	30	23-37, NR, 43% F.	one-sample t-test	100%	100%
	Guzman et al, unpublished	left	bilateral	bilateral	left	SD	198	18-30, 23±3, 73% F.	one-sample t-test	100%	100%

	Rojkova et al. 2016	bilateral#	bilateral#	-	bilateral#	SD	57	22-71, 45.45 ±14.79, 50% F.	summary stats based on unpaired t-test #	100%	100%
	Shu et al. 2015	-	-	bilateral	left	T-B	72	NR, 23.4±3.7, 42% F.	paired t-test	100%	79,2%
	Thiebaut de Schotten et al. 2011	-	bilateral	right	bilateral	T-B	40	18-22, NR, 50% F.	one-sample t-test	100%	100%
	Wu et al. 2016	-	bilateral	-	-	GQI	10	23-40, NR, 70% F.	paired t-test		
	This study	left	bilateral	bilateral	-	SD	172	22-36, 29.3±3.3, 61% F.	one-sample t-test	100%	98,26%
ILF	Latini et al. 2017	-	right	-	bilateral	T-B	24	21-28, NR, NR	unpaired t-test	100%	100%
	Shu et al. 2015	-	-	left	left	T-B	72	NR, 23.4±3.7, 42% F.	paired t-test	100%	79,2%
	Thiebaut de Schotten et al. 2011	-	bilateral	bilateral	left	T-B	40	18-22, NR, 50% F.	one-sample t-test	100%	100%

	This study	left	left	left	-	SD	172	22-36, 29.3±3.3, 61% F.	one-sample t-test	100%	98,26%
UF	Briggs et al. 2019	-	bilateral	-	-	GQI	10	23-34, 29.4±3.9, 60% F.#	unpaired t-test	NR	NR
	Guzman et al, unpublished	bilateral	right	right	bilateral	SD	198	18-30, 23±3, 73% F.	one-sample t-test	100%	100%
	Rojkova et al. 2016	bilateral#	bilateral#	-	right#	SD	57	22-71, 45.45 ±14.79, 50% F.	summary stats based on unpaired t-test #	100%	100%
	Shu et al. 2015	-	-	right	bilateral	T-B	72	NR, 23.4±3.7, 42% F.	paired t-test	100%	79,2%
	Thiebaut de Schotten et al. 2011	-	bilateral	bilateral	bilateral	T-B	40	18-22, NR, 50% F.	one-sample t-test	100%	100%
	This study	right	right	right	-	SD	172	22-36, 29.3±3.3, 61% F.	one-sample t-test	100%	98,26%
AFl	Catani et al. 2007	-	-	3 groups (majority left)	left	T-B	40	18-22, NR, 50% F.	one-sample t-test; k-means	100%	37,5%

	Guzman et al, unpublished	left	left	left	bilateral	SD	198	18-30, 23±3, 73% F.	one-sample t-test	100%	100%
	Rojkova et al. 2016	bilateral#	left #	-	right #	SD	57	22-71, 45.45 ±14.79, 50% F.	summary stats based on unpaired t-test #	94%	100%
	Thiebaut de Schotten et al. 2011	-	left	left	bilateral	T-B	40	18-22, NR, 50% F.	one-sample t-test	100%	40%
	This study	left	left	left	-	SD	172	22-36, 29.3±3.3, 61% F.	one-sample t-test	100%	98,26%
AFa	Catani et al. 2007	-	-	-	right	T-B	40	18-22, NR, 50% F.	one-sample t-test	100%	100%
	Guzman et al, unpublished	bilateral	right	right	bilateral	SD	198	18-30, 23±3, 73% F.	one-sample t-test	100%	100%
	Rojkova et al. 2016	right #	right #	-	right #	SD	57	22-71, 45.45 ±14.79, 50% F.	summary stats based on unpaired t-test #	100%	100%
	Thiebaut de Schotten et al. 2011	-	right	right	right	T-B	40	18-22, NR, 50% F.	one-sample t-test	100%	100%

	This study	right	right	right	-	SD	172	22-36, 29.3±3.3, 61% F.	one-sample t-test	100%	98,26%
AFp	Catani et al. 2007	-	-	-	NR	T-B	40	18-22, NR, 50% F.	one-sample t-test	100%	100%
	Thiebaut de Schotten et al. 2011	-	bilateral	bilateral	bilateral	T-B	40	18-22, NR, 50% F.	one-sample t-test	100%	100%
	This study	bilateral	left (marginal)	left (marginal)	-	SD	172	22-36, 29.3±3.3, 61% F.	one-sample t-test	100%	98,26%
AF	Shu et al. 2015	-	-	left	left	T-B	72	NR, 23.4±3.7, 42% F.	paired t-test	100%	79,2%
	Thiebaut de Schotten et al. 2011	-	right	bilateral	bilateral	T-B	40	18-22, NR, 50% F.	one-sample t-test	100%	100%

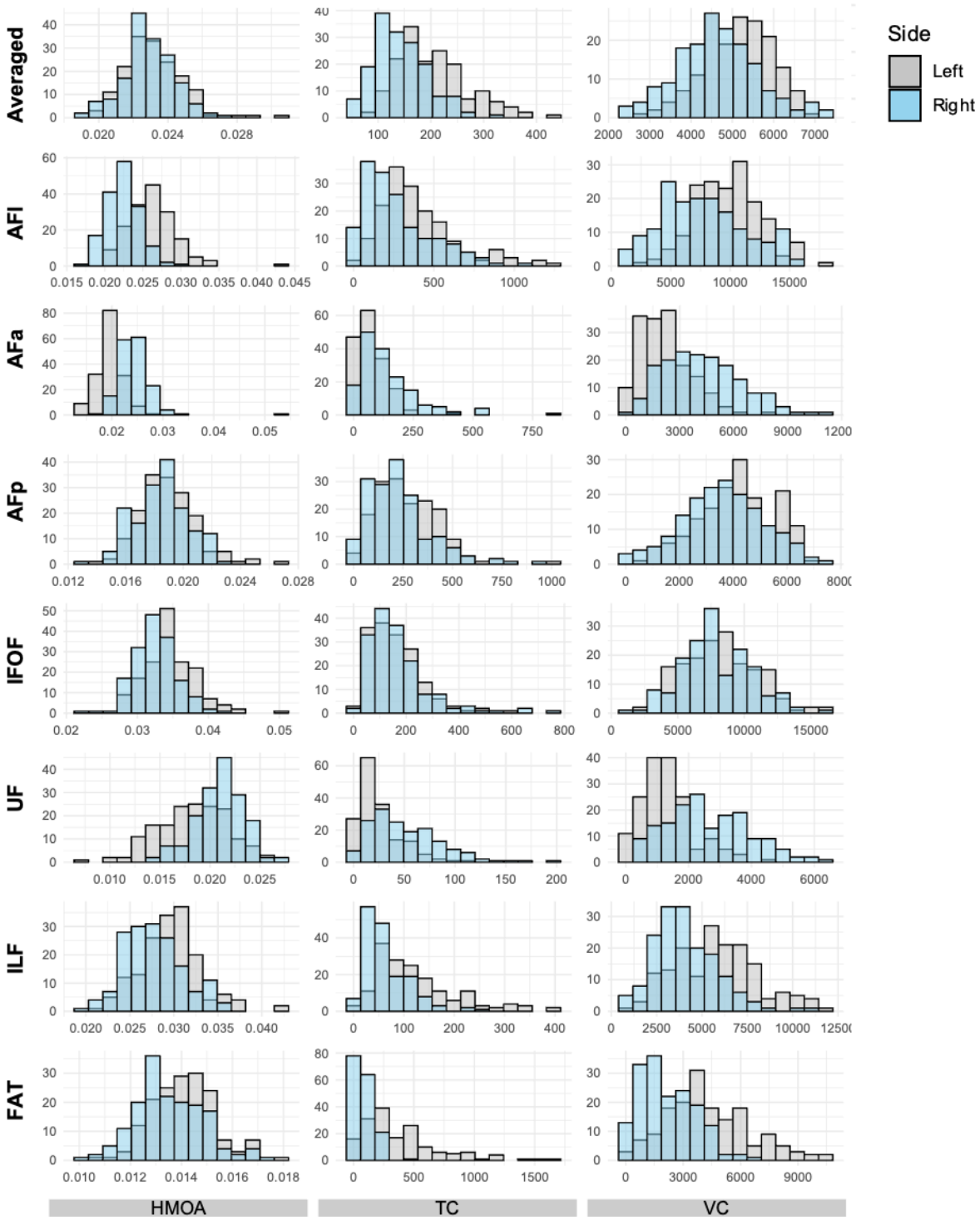

Figure 1. Distribution of raw tract-specific values for the left (light red) and right (light blue) hemispheres across participants. Each plot illustrates the respective metric's interindividual spread and central tendency, highlighting hemispheric differences in the magnitude and variability of white matter properties.

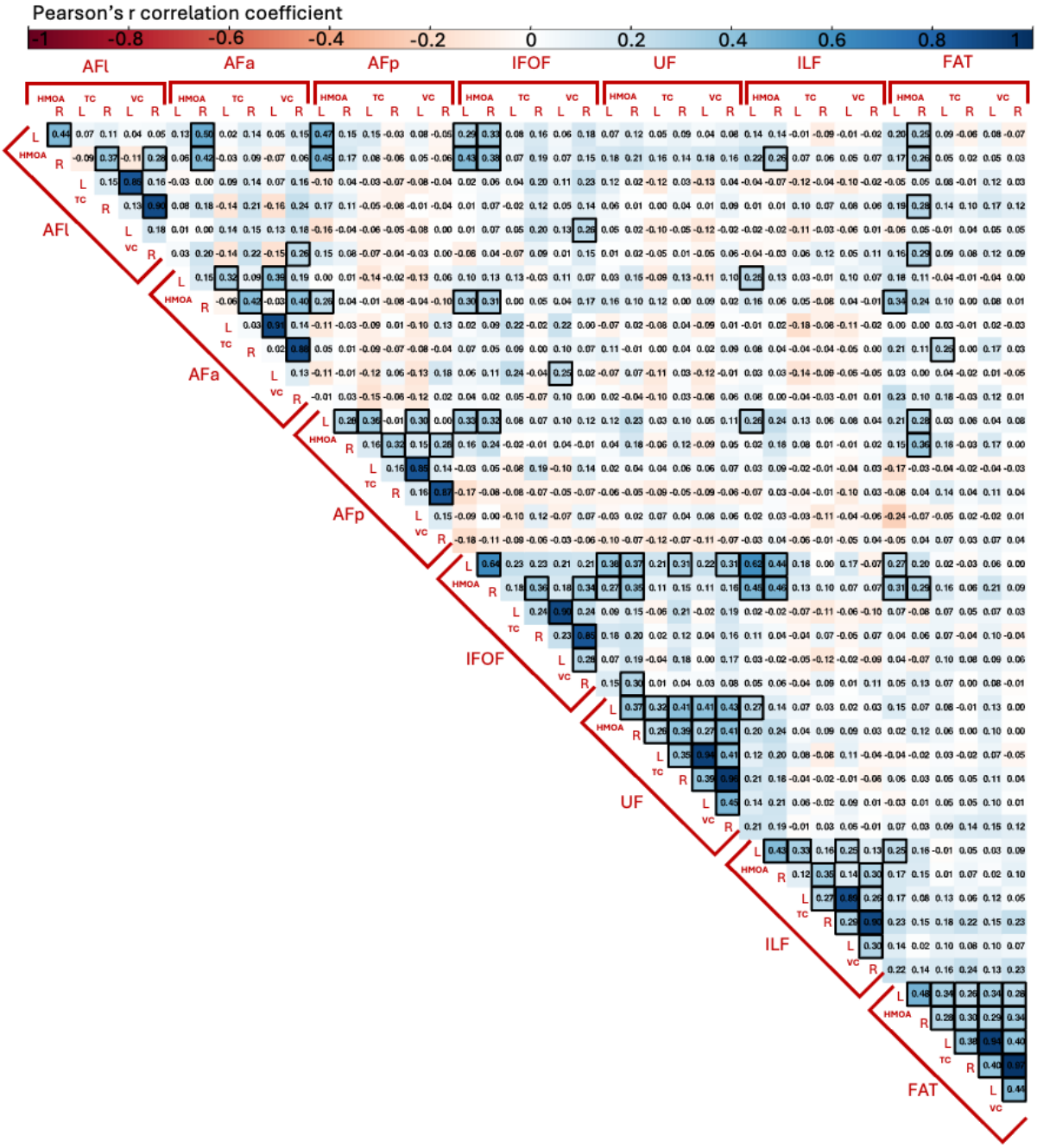

Figure 2. Correlation matrix of raw structural metrics (voxel count, streamline count, and HMOA) across language-relevant tracts in each hemisphere. Voxel and streamline counts show strong positive correlations within tracts, indicating high metric agreement for tract size. In contrast, HMOA is only weakly correlated with volumetric measures, reflecting its distinct sensitivity to microstructural properties. Squares indicate significant correlations (Bonferroni-corrected).

To better understand consistency across structural metrics, we computed intercorrelations between voxel count, streamline count, and HMOA for each tract within each hemisphere (see Supplementary Figure 2). As expected, voxel count and streamline count were highly correlated within each tract and hemisphere (Bonferroni-corrected r values often > 0.95), indicating that these metrics largely capture the same anatomical variance, most likely reflecting overall tract size. In contrast, HMOA showed weak or no correlation with either voxel or streamline count across tracts ($r \approx 0$ to 0.3), suggesting it reflects a distinct microstructural property (e.g., fibre integrity or

orientation dispersion) that is not reducible to tract volume. This dissociation helps explain why lateralisation and behavioural correlations involving HMOA may diverge from those based on voxel or streamline count and supports the inclusion of all three metrics in analyses aiming to disentangle size-based and microstructural contributions to function.

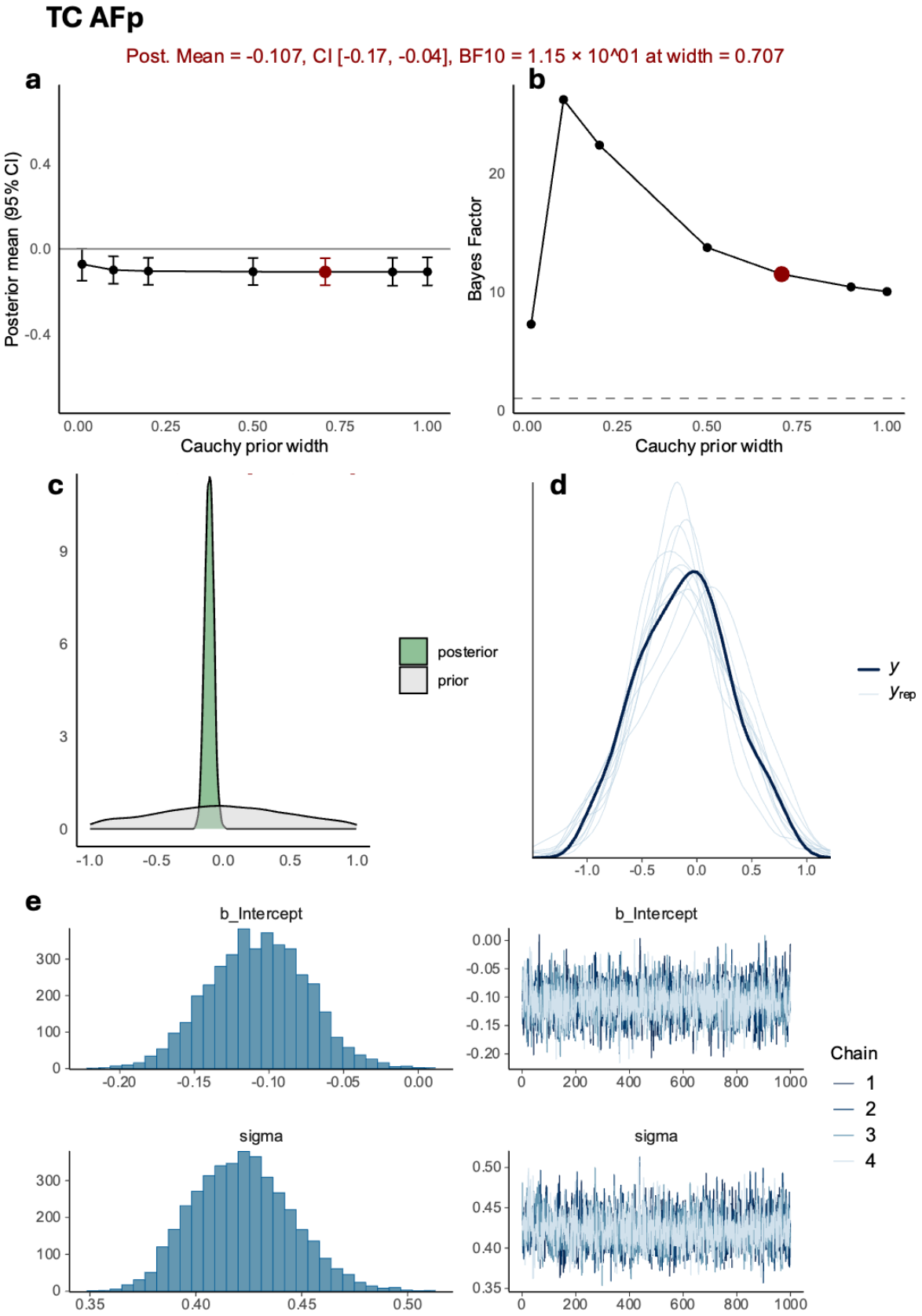
TC AFp
Post. Mean = -0.107, CI [-0.17, -0.04], BF10 = 1.15 × 10^01 at width = 0.707
a
Posterior mean (95% CI)
Cauchy prior width
b
Bayes Factor
Cauchy prior width
c
posterior
prior
d
y
y_rep
e
b_Intercept
b_Intercept
sigma
sigma
Chain
1
2
3
4

Figure 3. Robustness, posterior predictive checks, and convergence diagnostics for Bayesian lateralisation models. This is an example for the posterior arcuate fasciculus (pAF). Similar figures were generated for all 21 tract x metric combinations, each following the same processing and visualization pipeline, and are available in the Radboud Data Repository folder "Data_analysis/results/Bayesian/Lateralisation" (https://doi.org/10.34973/e0fm-pr30). (a) Posterior mean estimates (±95% credible intervals) across varying Cauchy prior widths. The posterior mean at chosen width = 0.707 (highlighted in red) was −0.107 (95% CI [−0.17, −0.04]). This plot shows how the estimated effect (posterior mean) changes depending on the prior width. The red point highlights the chosen prior width (0.707), where the effect is negative and statistically meaningful. (b) Bayes Factor (BF_{10}) as a function of Cauchy prior width. At chosen width = 0.707, BF_{10} = 11.5 (red point). This plot shows how much evidence the data provides in favor of an effect (Bayes Factor). At 0.707, the Bayes Factor is about 11.5, which indicates moderate-to-strong evidence. However, compared to other metrics and tracts, where Bayes Factors ranged from 93463 up to 2.97 × 10^44, this value is much lower. (c) Prior (gray) and posterior (green) distributions of the parameter estimate, indicating a posterior shift toward negative values relative to the prior. The green distribution is the posterior (updated belief after seeing data), and the gray distribution is the prior (belief before data). The posterior is narrower and shifted left, suggesting a stronger belief in a negative effect. (d) Posterior predictive distributions across sampling chains, demonstrating overlap and consistency across four chains. Each line shows results from a different sampling chain. The overlap of chains suggests the results are stable and reliable. (e) Parameter diagnostics. Left: Histograms of posterior samples for the intercept (top) and sigma (bottom). Right: Trace plots for the intercept and sigma across iterations for four chains, showing good chain mixing and convergence. The histograms show the distribution of sampled values for key parameters, and the trace plots show how the chains evolved over time. The good mixing of chains suggests convergence and reliable inference.

Analysis 1: Frequentistic approach in white matter lateralisaiton

To assess the statistical significance of white matter lateralisation, we conducted one-sample t-tests comparing each tract's lateralisation index (LI) to zero (i.e. no lateralisation), similar to previous studies (Briggs et al. 2019; Latini et al. 2017; Thiebaut de Schotten et al. 2011). The alpha threshold was adjusted using Bonferroni correction, setting the significance level to 0.0024 (0.05/[7 tracts × 3 measures]).

Most tracts were strongly asymmetrical with a preference for the left hemisphere. This included the long segment of the arcuate fasciculus, the ILF, and the FAT across all white matter properties (i.e., HMOA, TC, VC; $p < 0.0024$, Figure A and Table A). The pathways with a right asymmetry include the uncinate fasciculus and the anterior segment of the arcuate fasciculus, which showed statistically significant rightward lateralisation in HMOA, TC, and VC ($p < 0.0024$; Table A and Figure B).

A less clear pattern was evident for the IFOF and the posterior segment of the arcuate fasciculus. The IFOF was significantly left lateralised for HMOA ($t(163) = -8.41$, $p < .0024$, $M = -0.028$, $SD = 0.043$, 99.8% *CI* [-0.038, -0.018], *Cohen's d* = -0.657), but bilateral for track count ($t(163) = -0.12$, $p = 0.9008$, $M = -0.004$, SD = 0.361, 99.8% CI [-0.091, 0.084], *Cohen's d* = -0.01) and voxel count ($t(163) = -1.5$, $p = 0.1359$, $M = -0.024$, $SD = 0.208$, 99.8% *CI* [-0.075, 0.026], *Cohen's d* = -0.117). The posterior segment of the arcuate fasciculus exhibited the opposite pattern. HMOA was bilateral ($t(163) = -2.83$, $p = 0.0052$, $M = -0.013$, $SD = 0.06$, 99.8% *CI* [-0.028, 0.001], *Cohen's d* = -0.221), but left lateralised for track count ($t(163) = -3.30$, $p = 0.001$, $M = -0.108$, $SD = 0.419$, 99.8% *CI* [-0.209, -0.007], *Cohen's d* = -0.258) and voxel count ($t(163) = -3.58$, $p = 0.0004$, $M = -0.081$, $SD = 0.291$, 99.8% *CI* [-0.152, -0.011], *Cohen's d* = -0.280). However, the upper bound of the confidence intervals track and voxel count for AFp approached zero (i.e., no lateralisation), meaning both are statistically close to being bilateral (see Figure B for the bootstrap analysis).

Table A. Results of the statistical analysis of lateralisation. Adjusted significance level = 0.0024 (0.05/[7 tracts × 3 measures]).

LI index	Tract	Df	T stats.	P value	Mean	SD	CI lower	CI upper	Cohen's d
HMOA	AFl	163	-18.13	p < 0.0024	-0.077	0.054	-0.09	-0.064	-1.416
TC	AFl	163	-7.27	p < 0.0024	-0.226	0.399	-0.322	-0.13	-0.568
VC	AFl	163	-7.49	p < 0.0024	-0.147	0.252	-0.208	-0.087	-0.585
HMOA	AFa	163	15.7	p < 0.0024	0.1	0.082	0.08	0.12	1.226
TC	AFa	163	6.72	p < 0.0024	0.245	0.467	0.132	0.358	0.524
VC	AFa	163	12.14	p < 0.0024	0.322	0.34	0.24	0.405	0.948
HMOA	AFp	163	-2.83	0.0052	-0.013	0.06	-0.028	0.001	-0.221
TC	AFp	163	-3.3	0.0012	-0.108	0.419	-0.209	-0.007	-0.258
VC	AFp	163	-3.58	0.0004	-0.081	0.291	-0.152	-0.011	-0.28
HMOA	IFOF	163	-8.41	p < 0.0024	-0.028	0.043	-0.038	-0.018	-0.657
TC	IFOF	163	-0.12	0.9008	-0.004	0.361	-0.091	0.084	-0.01
VC	IFOF	163	-1.5	0.1359	-0.024	0.208	-0.075	0.026	-0.117
HMOA	UF	163	9.8	p < 0.0024	0.073	0.096	0.05	0.097	0.765
TC	UF	163	11.13	p < 0.0024	0.324	0.373	0.234	0.414	0.869

VC	UF	163	14.26	p < 0.0024	0.327	0.293	0.256	0.397	1.113
HMOA	ILF	163	-6.62	p < 0.0024	-0.033	0.063	-0.048	-0.017	-0.517
TC	ILF	163	-9.57	p < 0.0024	-0.271	0.363	-0.359	-0.184	-0.747
VC	ILF	163	-8.32	p < 0.0024	-0.167	0.258	-0.229	-0.105	-0.65
HMOA	FAT	163	-6.03	p < 0.0024	-0.023	0.048	-0.034	-0.011	-0.471
TC	FAT	163	-20.84	p < 0.0024	-0.55	0.338	-0.632	-0.469	-1.628
VC	FAT	163	-14.05	p < 0.0024	-0.341	0.311	-0.416	-0.266	-1.097

AFl: long segment of arcuate fasciculus, AFa: anterior segment of arcuate fasciculus, AFp: posterior segment of arcuate fasciculus, IFOF: inferior fronto-occipital fasciculus, UF: uncinate fasciculus, ILF: inferior longitudinal fasciculus, FAT: frontal aslant tract, HMOA: hindrance modulated orientational anisotropy, Df: degrees of freedom, CI: 99.76% confidence interval (Bonferroni adjusted CI), SD: standard deviation, TC: track count, VC: voxel count

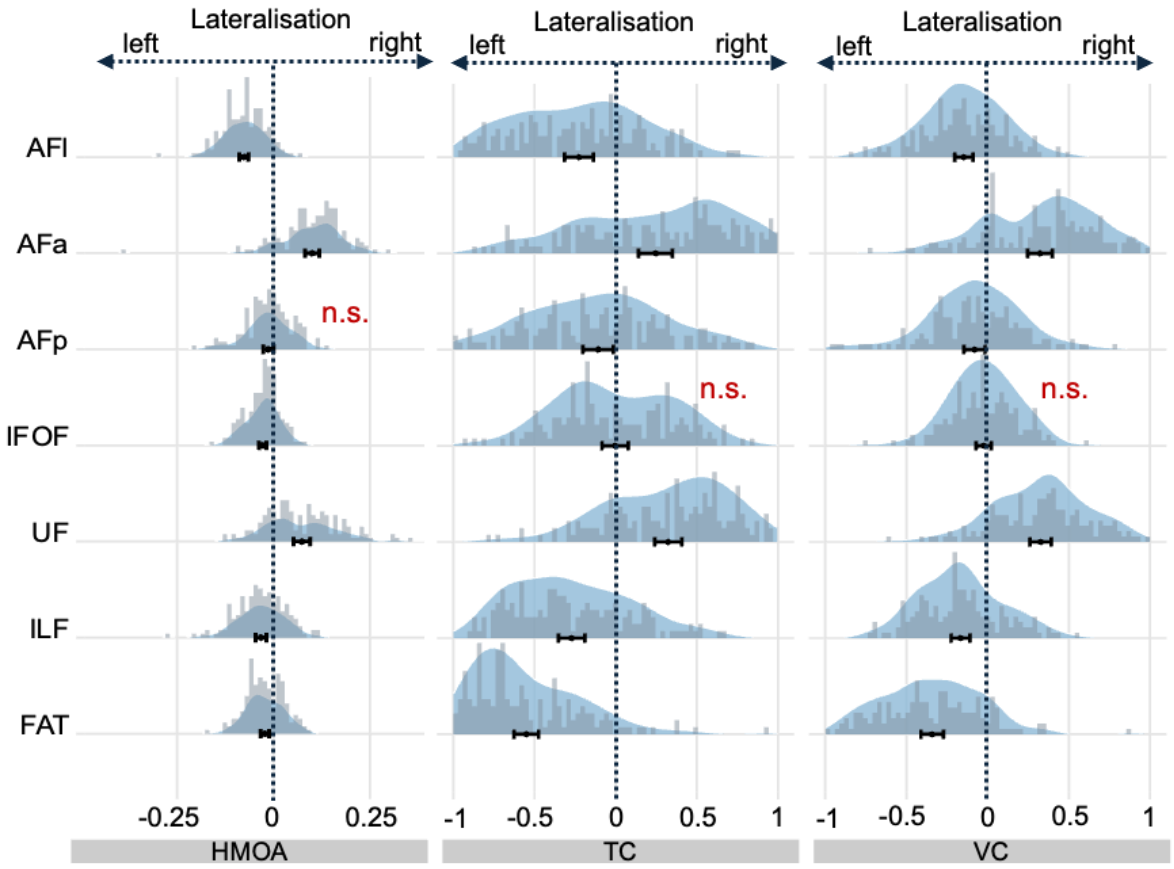

Figure A. Hemispheric asymmetry in language-recruited tracts across three white matter properties: hindrance modulated orientational anisotropy (HMOA), track count (TC), and voxel count (VC). The mean lateralisation index (LI) for each tract is plotted with Bonferroni-corrected 99.8% confidence intervals (n = 164). Grey histograms and overlaid blue density plots illustrate the distribution of LI values across participants. Negative LI values indicate leftward lateralisation; positive values indicate rightward lateralisation. AFl = long segment of the arcuate fasciculus; AFa = anterior segment of the arcuate fasciculus; AFp = posterior segment of the arcuate fasciculus; IFOF = inferior fronto-occipital fasciculus; UF = uncinate fasciculus; ILF = inferior longitudinal fasciculus; FAT = frontal aslant tract; n.s. = non-significant.

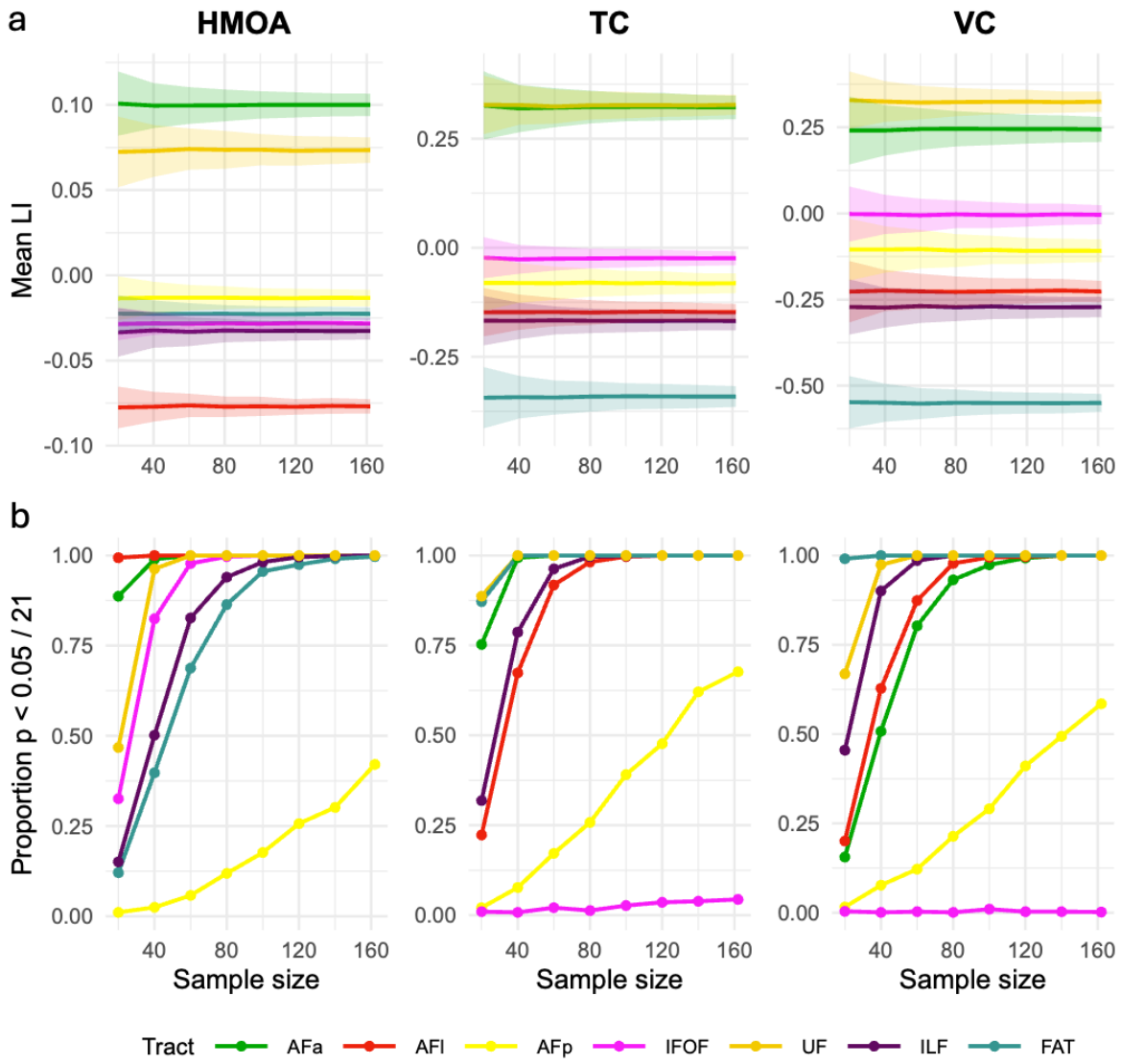

Figure B. Stability of tract-specific lateralisation as a function of sample size. a: Mean lateralisation index (LI) across 1,000 bootstrap resamples for each tract and metric, with shaded ribbons representing ±1 standard deviation. Increasing sample size reduces variability and stabilises LI estimates, revealing which tracts show robust lateralisation patterns at higher sample sizes. b: Proportion of significant lateralisation effects ($p < 0.05/21$) across the same bootstrap samples. Values >0.5 indicate that more than half of the samples showed a significant effect, reflecting consistent lateralisation beyond chance. Some tracts show reliable lateralisation even at smaller sample sizes, whereas others—such as AFp across several metrics—require larger samples for stable and statistically significant detection.

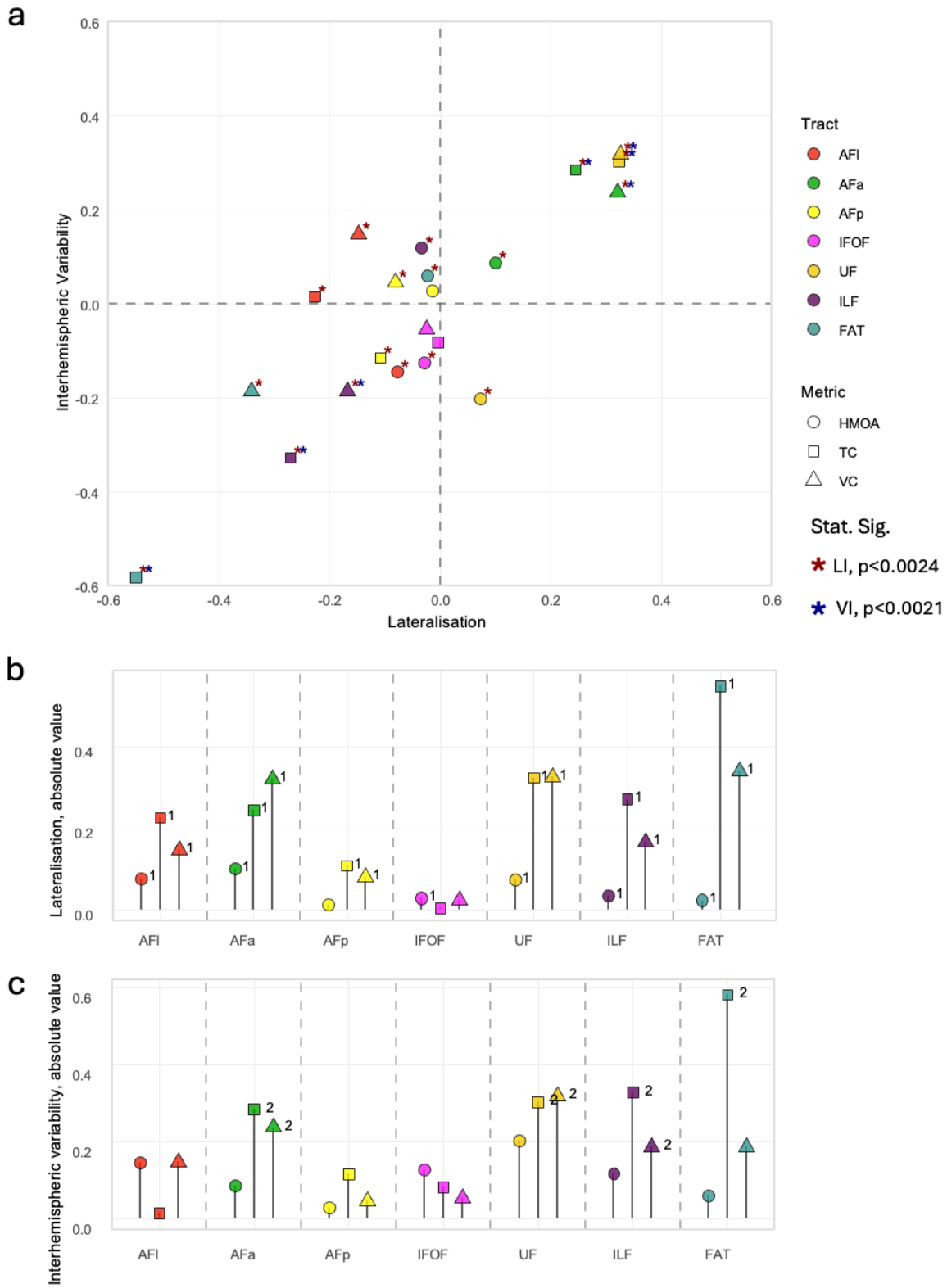

Figure C. Panel (a) shows a scatterplot illustrating the mean lateralisation and interhemispheric variability across tracts and metrics. Asterisks indicate statistically significant results after Bonferroni correction for lateralisation (dark red) and variability (dark blue) analyses. Panels (b) and (c) display the magnitude of lateralisation and interhemispheric variability, respectively, across tracts and metrics. The label/digit "1" denotes statistically significant results from the lateralisation analysis (within-tract, see Fig. A), and the label/digit "2" denotes significance from the variability analysis (within-tract, see Fig 2A from main analysis). AFl = long segment of the arcuate fasciculus; AFa = anterior segment, AFp = posterior segment, IFOF = inferior fronto-occipital

fasciculus; UF = uncinate fasciculus, ILF = inferior longitudinal fasciculus, FAT = frontal aslant tract, HMOA = hindrance modulated orientational anisotropy, TC = track count, VC = voxel count, LI = lateralisation index, VI = variability index.

Handedness and Structural Lateralisation

To assess whether handedness is correlated with white matter lateralisation in the seven language-related tracts, we calculated Pearson's correlation coefficients between the laterality indices of each tract and hand preference per participant, as measured by the Edinburgh Handedness Inventory (EHI; Oldfield, 1971). Bonferroni correction was applied to account for multiple comparisons. No significant correlations were observed after Bonferroni correction for multiple comparisons ($\alpha = 0.0024$; see Figure C).

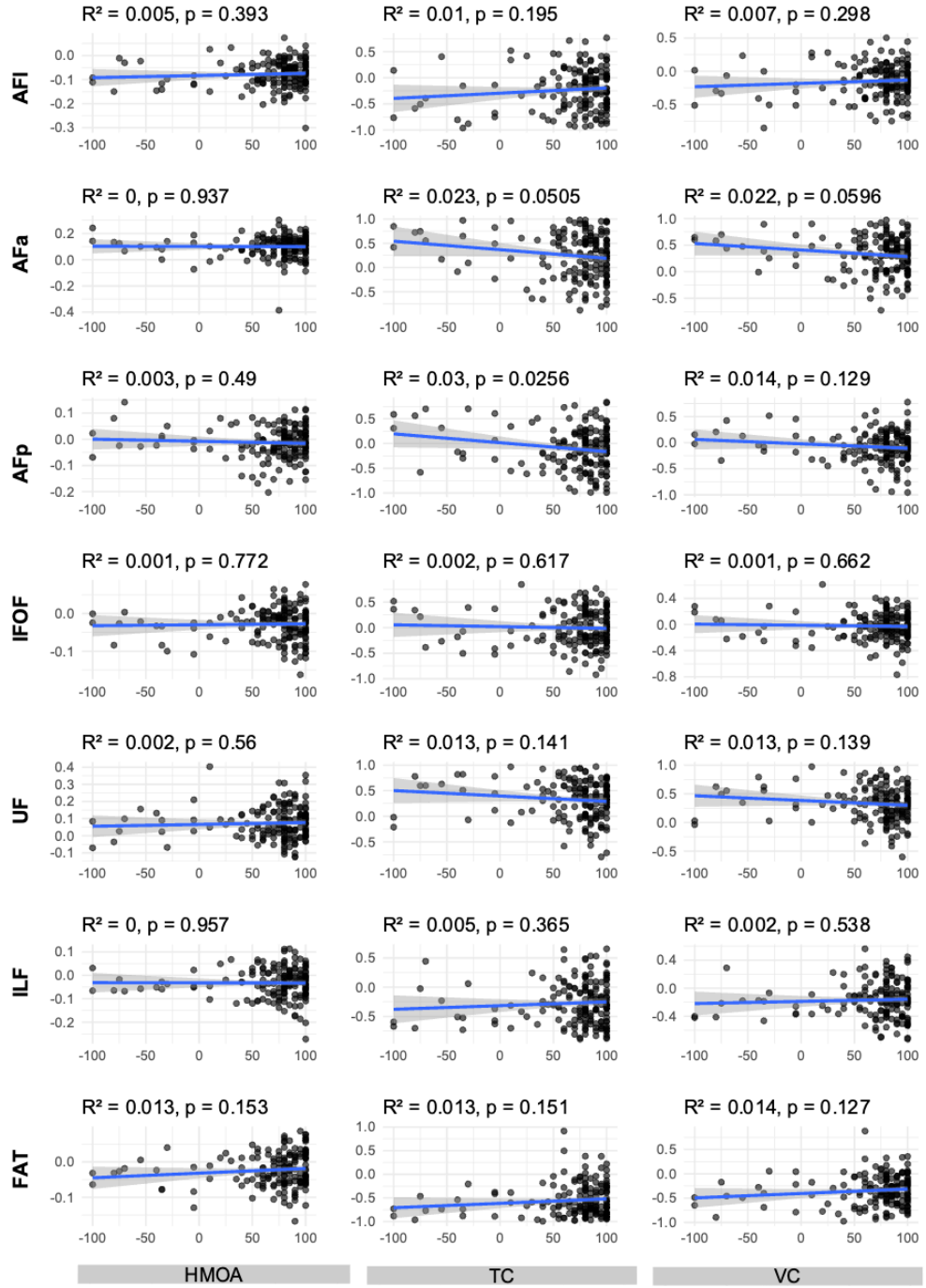

Figure D. Correlation between Edinburgh Handedness Inventory (EHI) scores and lateralisation indices (LI) of seven language-recruited tracts. Each plot shows the relationship between individual handedness scores and tract LI values. Significance was Bonferroni-corrected for multiple comparisons ($\alpha = 0.05/21 = 0.0024$). Most participants were right-handed (87%), 3.5% left-handed, and 9.9% ambidextrous. No significant correlations were observed after correction, suggesting that handedness, as indexed by EHI, does not systematically predict structural lateralisation in these language-recruited tracts.

Structural-Functional analysis

We assessed the relationship between structural lateralisation of language-relevant white matter tracts and performance on four language tasks from the NIH Toolbox and Human Connectome Project: Language Processing (accuracy and median reaction time), Picture Vocabulary (audio - picture matching), Oral Reading Recognition Test (visual word decoding), and Tone Discrimination (see Figure D). For each tract, we computed Pearson's correlation coefficients between the lateralisation index (LI) and behavioural performance across individuals. To control for multiple comparisons across tracts and tasks, we applied false discovery rate (FDR) correction.

The strongest association in this analysis emerged for the frontal aslant tract (FAT), where greater leftward lateralisation—based on voxel and track count—was linked to faster reaction times in the Language Processing task (VC and TC: $r = –0.19$), higher accuracy in Picture Vocabulary (VC: $r = 0.17$, TC: $r = 0.18$), and Oral Reading Recognition tasks (VC and TC: $r = 0.15$. Within the arcuate fasciculus, lateralisation indices based on voxel count and track count showed negligible linear associations with the selected language tasks across all three segments ($–0.10 < r < 0.10$). In contrast, HMOA-based lateralisation indices across the three segments showed moderate associations, including negative linear relation with Picture Vocabulary (AFl: $r = –0.18$; AFp: $r = –0.12$) and the Oral Reading Recognition tasks (AFa: $r = –0.15$).

In the ventral stream, the uncinate fasciculus (UF) showed opposing effects across tasks: rightward lateralisation correlated negatively with comprehension accuracy (VC and TC: $r = –0.13$) and was positively associated with Noise Discrimination test (VC and TC: $r = 0.11$). The inferior longitudinal fasciculus (ILF) showed a weak positive link with Oral Reading Recognition test performance (HMOA: $r = 0.10$) but negative correlation with the reaction time in language processing task (VC: $r = -0.13$, TC: $r = -0.11$). As opposed to FAT, the voxel count and track count of the IFOF was negatively correlated with Picture Vocabulary and Oral Reading Recognition tasks (TC: $r = -0.15$).

However, it is important to note that although several of these associations (i.e., those with $r \geq 0.17$ and $r \leq -0.17$) reached nominal significance ($p < 0.05$), none remained statistically significant after controlling for multiple comparisons using false discovery rate (FDR) correction.

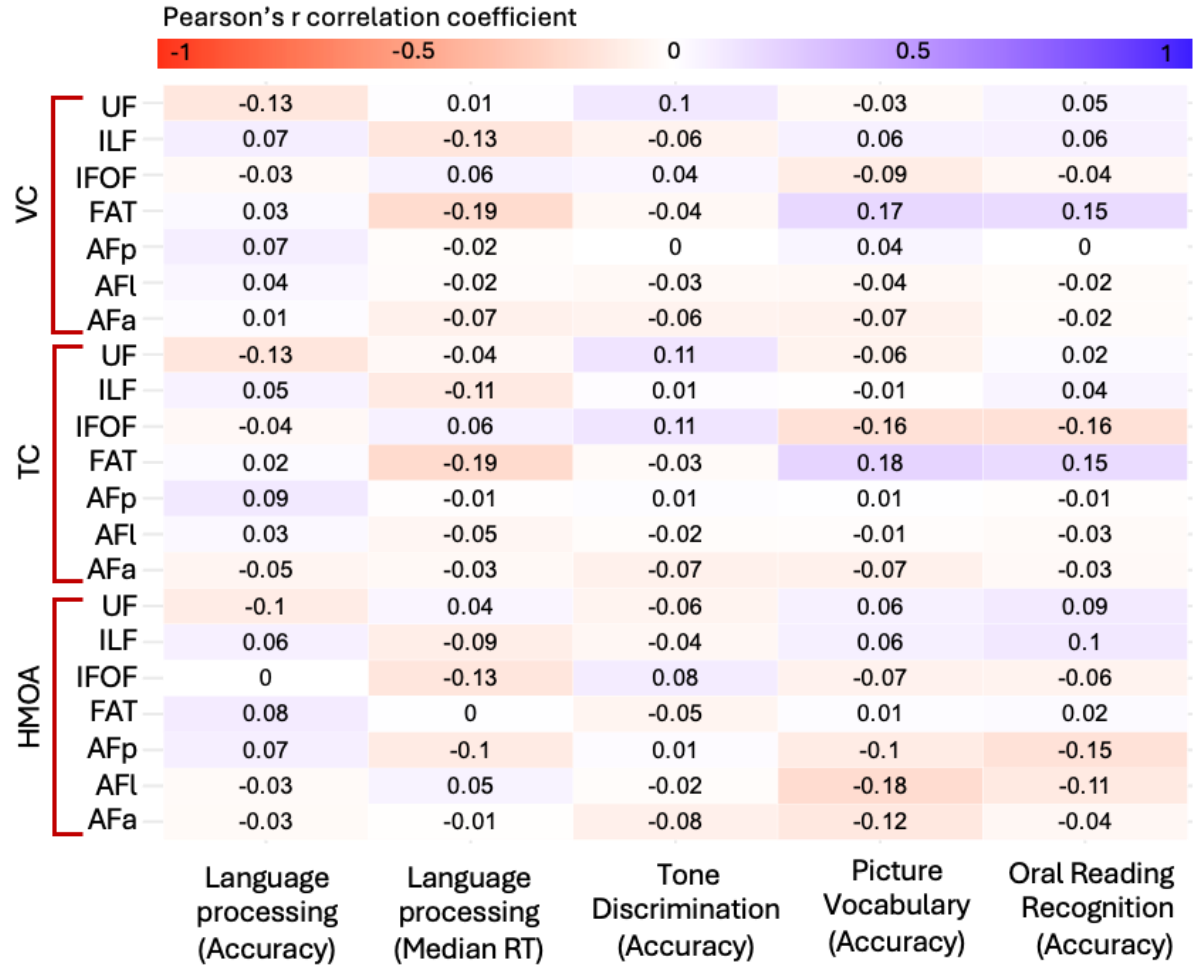

Figure E. Heatmap of correlations (Pearson's correlation coefficient, r) between language-related tasks from the Human Connectome Project and lateralisation metrics of language-recruited white matter tracts. No associations remained significant after false discovery rate (FDR) correction for multiple comparisons. RT: reaction time, AFl: long segment of arcuate fasciculus, AFa: anterior segment of arcuate fasciculus, AFp: posterior segment of arcuate fasciculus, IFOF: inferior fronto-occipital fasciculus, UF: uncinate fasciculus, ILF: inferior longitudinal fasciculus, FAT: frontal aslant tract, HMOA: hindrance modulated orientational anisotropy, TC: track count, VC: voxel count

Note 1: Functional relevance and clinical implications of language-recruited white matter tracts

Arcuate Fasciculus (three segments)

Konstantin Von Monkow was the first to link the arcuate fasciculus with language processes which was later incorporated in the Wernicke's model (Catani and Mesulam 2008; Dick and Tremblay 2012). Since then, a significant amount of research has been conducted to explore the role of the arcuate fasciculus in language (Ivanova et al. 2016; 2021; Kargar and Jalilian 2024). According to a systematic review by Forkel et al. (2022), the long segment of the arcuate fasciculus emerged as the most frequent tract associated with language processes. For instance, the long segment plays a role in word learning (López-Barroso et al. 2013). In contrast, the posterior and anterior segments of the arcuate fasciculus are predominantly discussed in the context of attention and memory (Forkel et al. 2022). However, it is essential to note that there is substantial evidence indicating that both the anterior and posterior segments of the arcuate fasciculus are closely intertwined with language processes. For instance, research by Thiebaut de Schotten et al. (2014) demonstrated changes in white matter microstructure within the posterior segment during literacy acquisition, which is consistent with a study by Ng et al. (2021). In their research, the disconnection of the posterior arcuate fasciculus resulted in alexia (Ng et al. 2021). Additionally, deficits in repetition among patients with primary progressive aphasia were shown to correlate with the reduced volume of the posterior segment (Forkel et al. 2020). In contrast, alterations in the anterior segment were associated with speech rate (Forkel et al. 2020). These findings are consistent with the results reported by Fridriksson et al. (2013) who studied 64 chronic left hemisphere stroke patients and demonstrated that the anterior segment correlated with decreased speech fluency (Fridriksson et al. 2013). However, Ivanova et al. (2021) reported no significant correlations between the volume and HMOA of the anterior segment and language processes, as assessed through various language-related tasks, including composite score fluency (Ivanova et al. 2021). Research is still needed to clarify the role of different segments of the left arcuate fasciculus. Hence, studying the left arcuate fasciculus and its segments remains an ongoing and multifaceted research endeavour. This complexity primarily arises from various paradigms, various tests and assessment methods, differences in dissection techniques, and individual variability across populations.

Recent work by Basile et al. (2024) advances this segmentation framework by combining diffusion tractography and resting-state fMRI to uncover a tripartite functional parcellation of the frontotemporal arcuate fasciculus (Basile et al. 2024). Using a hybrid method known as track-weighted dynamic functional connectivity, they identified ventral, middle, and dorsal AF clusters that show distinct patterns of functional connectivity and meta-analytic term associations. The ventral cluster was linked to phonological and auditory processing (e.g., pitch, voice), the middle cluster to semantic integration and higher-order language functions, and the dorsal cluster to non-linguistic cognitive domains. Notably, these findings support a morpho-functional dissociation within the AF that refines classic dual-stream models by showing how subsegments of the arcuate support distinct aspects of language production and comprehension. In addition, the observation that the middle segment of the right arcuate is particularly implicated in social communication and mentalising (Basile et al. 2024), potentially points to a possible dissociation between affective-pragmatic and core linguistic processing streams.

While research on the left arcuate fasciculus has been a central focus since the 19th century, the exploration of the right hemisphere, particularly the right arcuate fasciculus, is still in its early stages and has not been studied as extensively as its left hemisphere counterpart (Thiebaut de Schotten et al. 2020). There is growing

evidence supporting the hypothesis about the role of the right arcuate fasciculus as a potential compensatory tract following damage to the left hemisphere (Chupina et al. 2022; Forkel, Thiebaut de Schotten, Dell'Acqua, et al. 2014; Kourtidou et al. 2021; Pani et al. 2016; Riès et al. 2016; but see Geva et al. 2015). Such compensatory reorganisation aligns with frameworks of functional degeneracy, whereby multiple structural pathways can support overlapping cognitive functions, particularly in the context of recovery or developmental adaptation (Price and Friston 2002). In developmental disorders, the high integrity of the right arcuate correlates with better language performance (Paldino et al. 2016). Nonetheless, aphasia can also occur after right hemisphere strokes in right-handed individuals, implying that the right hemisphere in those patients plays a significant role in language processes even before stroke. This phenomenon, crossed aphasia, has been documented in several studies (Alexander and Annett 1996; Dewarrat et al. 2009). Even if we consider these cases as "atypical" in terms of language lateralisation, there is evidence for the right hemisphere's involvement in language processes such as prosody (Sheppard et al. 2020) and affective language (Blake et al. 2002). The importance of the right hemisphere in language was discussed by the pioneering neurologist Hughlings Jackson a decade after Broca's publication (Hughlings Jackson 1874). Jackson's theory of language encompassed both intellectual or voluntary and emotional or automatic language, with the latter being primarily supported by the right hemisphere and preserved in patients with aphasia (Hughlings Jackson 1879; 1874). Further research on automatic and emotional language has the potential to enhance our understanding of involuntary, automatic and emotional speech in patients with Tourette's syndrome (Lanser et al. 1993; Yang et al. 2021), preserved ability to sing in patients with language disorders (Schlaug et al. 2008), language deficits in schizophrenia (Mitchell and Crow 2005). However, it remains unclear whether the right arcuate fasciculus, among all the white matter tracts related to language in the right hemisphere, plays a dominant role in these language processes.

In summary, the functional roles of the arcuate fasciculus and its segments remain topics of ongoing research and debate. There is a growing interest in the role of the right hemisphere in language and the arcuate fasciculus, both in terms of its potential to compensate for language dysfunction following left hemisphere stroke and its inherent involvement in language functions. Whether these segmental roles generalise across language typologies or reflect experience-dependent plasticity remains to be fully tested, particularly in tonal, agglutinative, or signed languages.

Inferior Fronto-Occipital Fasciculus

The IFOF is a white matter tract that connects the ventro-medial occipital cortex with the polar and orbital frontal cortex (Forkel, Thiebaut de Schotten, Kawadler, et al. 2014). Research has established the left IFOF's crucial role in language processes, with studies demonstrating its involvement in both verbal and non-verbal semantic functions. (Almairac et al. 2015; Duffau et al. 2005; but see Giampiccolo et al. 2025).

Almairac et al. (2015) found that patients with greater infiltration of the left IFOF by diffuse low-grade glioma showed significantly poorer performance on semantic fluency tasks compared to phonological fluency tasks, though these patients also presented with both semantic and phonological paraphasias during intraoperative axonal stimulation. Extending beyond verbal tasks, Moritz-Gasser et al. (2013) demonstrated the left IFOF's involvement in non-verbal semantic processes, specifically in matching pictures from the same category across different input modalities (verbal, visual, and auditory). Notably, stimulation of the left IFOF during surgery induced anosognosia, leaving patients unaware of their errors, a finding that aligns with (Pacella et al. 2020), who

reported that damage to 30% of the left IFOF (among other tracts) was associated with anosognosia following traumatic brain injury.

While the left hemisphere's dominance in semantic processing has been well-established, recent evidence suggests a more nuanced picture of lateralisation. Herbet et al. (2017) challenged conventional understanding by demonstrating that stimulation of the right IFOF during awake brain surgery also impacted patients' non-verbal semantic processes. This finding suggests bilateral involvement in semantic processing, though the authors noted that their results do not exclude the right IFOF's potential role in verbal semantic processes, as some patients exhibited verbal semantic paraphasias during picture naming tasks.

Collectively, these findings indicate that the Inferior Fronto-Occipital fasciculus contributes to both verbal and non-verbal semantic processes across both hemispheres, suggesting a more distributed model of semantic processing than traditionally conceived.

Uncinate Fasciculus

The role of the left UF has predominantly been explored in the context of psychiatric disorders (Craig et al. 2009; Forkel et al. 2022). In language, the function of the UF remains a subject of extensive debate (for the discussion, see Von Der Heide et al. 2013). Evidence from direct electrical stimulation of the UF during awake surgery in patients with low-grade glioma has not been shown to induce semantic paraphasias or picture naming errors (Duffau et al. 2009). However, a lesion study by Catani et al. (2013) demonstrated that the degeneration of the left UF in primary progressive aphasia was correlated with the performance on picture naming tasks, such as the Boston Naming Task, while abnormalities in the Frontal Aslant Tract were linked to verbal fluency (Catani et al., 2013). Other lesion studies report that the retrieval of proper names of individuals was associated with both the left UF (Papagno et al. 2011; 2016) and the cortical regions connected by the left UF (Giussani et al. 2011). Two extensive systematic reviews, conducted by Von Der Heide et al. (2013) and Cocquyt et al. (2020), raised doubts about the role of the left UF in general semantic processes. On the contrary, recent diffusion study has indicated that the right UF is implicated in phonological and lexical-semantic verbal short-term memory abilities (Olivé et al. 2023).

In summary, the Uncinate Fasciculus has been functionally associated with naming abilities, although it's important to note that some controversies persist. Furthermore, the role of UF anatomical asymmetry remains a topic for future research.

Inferior Longitudinal Fasciculus

The left and right ILFs appear to display chameleon-like behaviour. Their role in various functions depends on the condition or context, such as a behavioural task chosen by the researcher. An extensive review by Herbet et al. (2018) demonstrated that in the literature, the ILF has been linked to face recognition, emotions, visual memory, semantic and lexical processes, object recognition, and reading (Herbet et al. 2018). Most of these functions were proposed in the original description of its anatomy using tractography (Catani et al. 2003).

Regarding the role of the hemispheric specialisation of the ILF in language processes (e.g., reading), it is not yet clear if only the left ILF is recruited during language-related tasks. For example, Horowitz-Kraus et al. (2014) demonstrated that the mean FA values of the right ILF significantly correlated with the ability to read words fluently, while the mean FA of the right AF was associated with reading comprehension (Horowitz-Kraus et al. 2014). However, Feldman et al. (2012) showed a negative correlation between the FA values of the right ILF and reading comprehension (Feldman et al. 2012). In contrast, Thiebaut de Schotten et al. (2014) found no

significant correlation between reading performance and the FA values of the ILF in both hemispheres (Thiebaut de Schotten et al. 2014).

In summary, the Inferior Longitudinal Fasciculus has been functionally implicated in a wide array of cognitive processes—from reading to emotion and object recognition—with emerging evidence suggesting its role may be flexibly modulated by task demands and hemispheric specialisation.

Frontal Aslant Tract

Due to the FAT's connection between pre- and supplementary motor regions with the inferior frontal gyrus in the left hemisphere (Catani et al. 2012), researchers have been exploring the role of the FAT in language (Dick et al. 2019). Awake electrical stimulation of the left FAT in patients with frontal lobe glioma leads to temporary speech arrest or speech inhibition deficits (Fujii et al. 2015; Kinoshita et al. 2015; Vassal et al. 2014), with Kemerdere et al. (2016) demonstrating that axonal stimulation can induce stuttering, eventually progressing to mutism or speech arrest. While these findings provide valuable evidence for researchers, one should be cautious when inferring the specific role of the FAT in language, primarily for several key reasons

First, these studies establish associations between symptoms (i.e., stuttering) and FAT stimulation rather than demonstrating causation, as Jackson noted: "To locate the damage which destroys speech and to locate speech are two different things" . The stimulation findings reveal associations, but more robust theories require dissociations, ideally double-dissociations (Caplan 2018). Notably, speech arrest also occurs with direct electrical stimulation of other tracts, including the left uncinate fasciculus (Papagno et al. 2011) and the anterior segment of the arcuate fasciculus (Duffau et al. 2002). Given that these tracts are interconnected components of a broader network with nearby terminations (Mandonnet et al. 2010), stimulating one tract may disrupt another involved in speech initiation. Second, distinguishing between articulatory (motor) dysfunction and higher-order speech dysfunction (propositioning, ordering words in meaningful sentences) remains challenging, requiring new testing paradigms to disentangle these interpretations from awake surgery studies.

Neuroimaging studies using diffusion tensor imaging have begun to provide clearer dissociations. Catani et al. (2013) demonstrated that in patients with primary progressive aphasia, abnormalities in the left FAT correlated with verbal fluency deficits but not with naming or semantic processing, while the uncinate fasciculus showed the opposite pattern. However, Landers et al. (2022) found significant correlations between the right FAT's microstructural indices and letter fluency in glioma patients, with no such correlations for the left FAT. Similarly, Neef et al. (2018) identified reduced fractional anisotropy in the right FAT (alongside bilateral Superior Longitudinal Fasciculus changes) in adults who stutter compared to controls.

This bilateral complexity is further illustrated by Vallesi and Babcock's (2020) findings in healthy individuals, where greater leftward lateralisation of the FAT correlated with faster lexical decision-making but showed no relationship with verbal fluency performance (Vallesi and Babcock 2020). Collectively, these neuroimaging findings suggest that while the FAT contributes to speech initiation and fluency, its role varies across different linguistic processes and involves complex bilateral interactions.

In summary, the Frontal Aslant Tract appears central to speech initiation and fluency, but the mechanisms underlying speech disruption and the specific contributions of hemispheric asymmetry represent important areas for future research. The emerging picture suggests a nuanced role that cannot be reduced to simple unilateral language dominance models.

Supplementary References

Alexander, M. P., and M. Annett. 1996. “Crossed Aphasia and Related Anomalies of Cerebral Organization: Case Reports and a Genetic Hypothesis.” *Brain and Language* 55 (2): 213–39. https://doi.org/10.1006/brln.1996.0102.

Almairac, Fabien, Guillaume Herbet, Sylvie Moritz-Gasser, Nicolas Menjot de Champfleur, and Hugues Duffau. 2015. “The Left Inferior Fronto-Occipital Fasciculus Subserves Language Semantics: A Multilevel Lesion Study.” *Brain Structure and Function* 220 (4): 1983–95. https://doi.org/10.1007/s00429-014-0773-1.

Baarsen, K. M. van, M. Kleinnijenhuis, S. Jbabdi, S. N. Sotiropoulos, J. A. Grotenhuis, and A. M. van Cappellen van Walsum. 2016. “A Probabilistic Atlas of the Cerebellar White Matter.” *NeuroImage* 124 (January): 724–32. https://doi.org/10.1016/j.neuroimage.2015.09.014.

Basile, Gianpaolo Antonio, Victor Nozais, Angelo Quartarone, et al. 2024. “Functional Anatomy and Topographical Organization of the Frontotemporal Arcuate Fasciculus.” *Communications Biology* 7 (1): 1655. https://doi.org/10.1038/s42003-024-07274-3.

Blake, Margaret Lehman, Joseph R. Duffy, Penelope S. Myers, and Connie A. Tompkins. 2002. “Prevalence and Patterns of Right Hemisphere Cognitive/Communicative Deficits: Retrospective Data from an Inpatient Rehabilitation Unit.” *Aphasiology* (United Kingdom) 16 (4–6): 537–47. https://doi.org/10.1080/02687030244000194.

Briggs, Robert G., Arpan R. Chakraborty, Christopher D. Anderson, et al. 2019. “Anatomy and White Matter Connections of the Inferior Frontal Gyrus.” *Clinical Anatomy (New York, N.Y.)* 32 (4): 546–56. https://doi.org/10.1002/ca.23349.

Caplan, Bruce. 2018. “Double Dissociation.” In *Encyclopedia of Clinical Neuropsychology*. Springer, Cham. https://doi.org/10.1007/978-3-319-57111-9_9280.

Catani, Marco, Matthew P.G. Allin, Masud Husain, et al. 2007. “Symmetries in Human Brain Language Pathways Correlate with Verbal Recall.” *Proceedings of the National Academy of Sciences of the United States of America* 104 (43): 17163–68. https://doi.org/10.1073/pnas.0702116104.

Catani, Marco, Flavio Dell’Acqua, Francesco Vergani, et al. 2012. “Short Frontal Lobe Connections of the Human Brain.” *Cortex* 48 (2): 273–91. https://doi.org/10.1016/j.cortex.2011.12.001.

Catani, Marco, Robert J. Howard, Sinisa Pajevic, and Derek K. Jones. 2002. “Virtual in Vivo Interactive Dissection of White Matter Fasciculi in the Human Brain.” *NeuroImage* 17 (1): 77–94. https://doi.org/10.1006/nimg.2002.1136.

Catani, Marco, Derek K. Jones, Rosario Donato, and Dominic H. Ffytche. 2003. “Occipito-Temporal Connections in the Human Brain.” *Brain* 126 (9): 2093–107. https://doi.org/10.1093/brain/awg203.

Catani, Marco, and Marsel Mesulam. 2008. “The Arcuate Fasciculus and the Disconnection Theme in Language and Aphasia: History and Current State.” *Cortex; a Journal Devoted to the Study of the Nervous System and Behavior* 44 (8): 953–61. https://doi.org/10.1016/j.cortex.2008.04.002.

Catani, Marco, Marsel M. Mesulam, Estrid Jakobsen, et al. 2013. “A Novel Frontal Pathway Underlies Verbal Fluency in Primary Progressive Aphasia.” *Brain: A Journal of Neurology* 136 (Pt 8): 2619–28. https://doi.org/10.1093/brain/awt163.

Catani, Marco, and Michel Thiebaut de Schotten. 2008. “A Diffusion Tensor Imaging Tractography Atlas for Virtual in Vivo Dissections.” *Cortex* 44 (8): 1105–32. https://doi.org/10.1016/j.cortex.2008.05.004.

Chupina, Irina, Joanna Sierpowska, Xiaochen Y. Zheng, Anna Dewenter, Maria-Carla Piastra, and Vitória Piai. 2022. “Time Course of Right-Hemisphere Recruitment during Word Production Following Left-

Hemisphere Damage: A Single Case of Young Stroke." *The European Journal of Neuroscience* 56 (8): 5235–59. https://doi.org/10.1111/ejn.15813.

Cocquyt, E. -M., E. Lanckmans, P. van Mierlo, et al. 2020. "The White Matter Architecture Underlying Semantic Processing: A Systematic Review." *Neuropsychologia* 136 (January): 107182. https://doi.org/10.1016/j.neuropsychologia.2019.107182.

Craig, M. C., M. Catani, Q. Deeley, et al. 2009. "Altered Connections on the Road to Psychopathy." *Molecular Psychiatry* 14 (10): 946–53, 907. https://doi.org/10.1038/mp.2009.40.

Dewarrat, Géraldine Maillard, Jean-Marie Annoni, Eleonora Fornari, Antonio Carota, Julien Bogousslavsky, and Philippe Maeder. 2009. "Acute Aphasia after Right Hemisphere Stroke." *Journal of Neurology* 256 (9): 1461–67. https://doi.org/10.1007/s00415-009-5137-z.

Dick, Anthony Steven, Dea Garic, Paulo Graziano, and Pascale Tremblay. 2019. "The Frontal Aslant Tract (FAT) and Its Role in Speech, Language and Executive Function." *Cortex; a Journal Devoted to the Study of the Nervous System and Behavior* 111 (February): 148–63. https://doi.org/10.1016/j.cortex.2018.10.015.

Dick, Anthony Steven, and Pascale Tremblay. 2012. "Beyond the Arcuate Fasciculus: Consensus and Controversy in the Connectional Anatomy of Language." *Brain: A Journal of Neurology* 135 (Pt 12): 3529–50. https://doi.org/10.1093/brain/aws222.

Duffau, Hugues, Laurent Capelle, Nicole Sichez, et al. 2002. "Intraoperative Mapping of the Subcortical Language Pathways Using Direct Stimulations: An Anatomo-functional Study." *Brain* 125 (1): 199–214. https://doi.org/10.1093/brain/awf016.

Duffau, Hugues, Peggy Gatignol, Emmanuel Mandonnet, Philippe Peruzzi, Nathalie Tzourio-Mazoyer, and Laurent Capelle. 2005. "New Insights into the Anatomo-Functional Connectivity of the Semantic System: A Study Using Cortico-Subcortical Electrostimulations." *Brain: A Journal of Neurology* 128 (Pt 4): 797–810. https://doi.org/10.1093/brain/awh423.

Duffau, Hugues, Peggy Gatignol, Sylvie Moritz-Gasser, and Emmanuel Mandonnet. 2009. "Is the Left Uncinate Fasciculus Essential for Language? A Cerebral Stimulation Study." *Journal of Neurology* 256 (3): 382–89. https://doi.org/10.1007/s00415-009-0053-9.

Feldman, Heidi M., Eliana S. Lee, Jason D. Yeatman, and Kristen W. Yeom. 2012. "Language and Reading Skills in School-Aged Children and Adolescents Born Preterm Are Associated with White Matter Properties on Diffusion Tensor Imaging." *Neuropsychologia* 50 (14): 3348–62. https://doi.org/10.1016/j.neuropsychologia.2012.10.014.

Forkel, Stephanie J., Patrick Friedrich, Michel Thiebaut de Schotten, and Henrietta Howells. 2022. "White Matter Variability, Cognition, and Disorders: A Systematic Review." *Brain Structure and Function* 227 (2): 529–44. https://doi.org/10.1007/s00429-021-02382-w.

Forkel, Stephanie J., Emily Rogalski, Niki Drossinos Sancho, et al. 2020. "Anatomical Evidence of an Indirect Pathway for Word Repetition." *Neurology* 94 (6): e594–606. https://doi.org/10.1212/WNL.0000000000008746.

Forkel, Stephanie J., Michel Thiebaut de Schotten, Flavio Dell'Acqua, et al. 2014. "Anatomical Predictors of Aphasia Recovery: A Tractography Study of Bilateral Perisylvian Language Networks." *Brain* 137 (7): 2027–39. https://doi.org/10.1093/brain/awu113.

Forkel, Stephanie J., Michel Thiebaut de Schotten, Jamie M. Kawadler, Flavio Dell'Acqua, Adrian Danek, and Marco Catani. 2014. "The Anatomy of Fronto-Occipital Connections from Early Blunt Dissections to Contemporary Tractography." *Cortex* 56: 73–84. https://doi.org/10.1016/j.cortex.2012.09.005.

Fridriksson, Julius, Dazhou Guo, Paul Fillmore, Audrey Holland, and Chris Rorden. 2013. "Damage to the Anterior Arcuate Fasciculus Predicts Non-Fluent Speech Production in Aphasia." *Brain: A Journal of Neurology* 136 (Pt 11): 3451–60. https://doi.org/10.1093/brain/awt267.

Fujii, Masazumi, Satoshi Maesawa, Kazuya Motomura, et al. 2015. “Intraoperative Subcortical Mapping of a Language-Associated Deep Frontal Tract Connecting the Superior Frontal Gyrus to Broca’s Area in the Dominant Hemisphere of Patients with Glioma.” *Journal of Neurosurgery* 122 (6): 1390–96. https://doi.org/10.3171/2014.10.JNS14945.

Geva, Sharon, Marta M. Correia, and Elizabeth A. Warburton. 2015. “Contributions of Bilateral White Matter to Chronic Aphasia Symptoms as Assessed by Diffusion Tensor MRI.” *Brain and Language* 150 (November): 117–28. https://doi.org/10.1016/j.bandl.2015.09.001.

Giampiccolo, Davide, Guillaume Herbet, and Hugues Duffau. 2025. “The Inferior Fronto-Occipital Fasciculus: Bridging Phylogeny, Ontogeny and Functional Anatomy.” *Brain* 148 (5): 1507–25. https://doi.org/10.1093/brain/awaf055.

Giussani, Carlo, Matteo Riva, Marcello Gallucci, et al. 2011. “Anatomical Correlates for Category-Specific Naming of Living and Non-Living Things.” *NeuroImage* 56 (1): 323–29. https://doi.org/10.1016/j.neuroimage.2011.01.080.

Guevara, Miguel, Claudio Román, Josselin Houenou, et al. 2017. “Reproducibility of Superficial White Matter Tracts Using Diffusion-Weighted Imaging Tractography.” *NeuroImage* 147 (February): 703–25. https://doi.org/10.1016/j.neuroimage.2016.11.066.

Guevara, P., D. Duclap, C. Poupon, et al. 2012. “Automatic Fiber Bundle Segmentation in Massive Tractography Datasets Using a Multi-Subject Bundle Atlas.” *NeuroImage* 61 (4): 1083–99. https://doi.org/10.1016/j.neuroimage.2012.02.071.

Hagler, Donald J., Mazyar E. Ahmadi, Joshua Kuperman, et al. 2009. “Automated White-Matter Tractography Using a Probabilistic Diffusion Tensor Atlas: Application to Temporal Lobe Epilepsy.” *Human Brain Mapping* 30 (5): 1535–47. https://doi.org/10.1002/hbm.20619.

Hansen, Colin B., Qi Yang, Ilwoo Lyu, et al. 2021. “Pandora: 4-D White Matter Bundle Population-Based Atlases Derived from Diffusion MRI Fiber Tractography.” *Neuroinformatics* 19 (3): 447–60. https://doi.org/10.1007/s12021-020-09497-1.

Herbet, Guillaume, Sylvie Moritz-Gasser, and Hugues Duffau. 2017. “Direct Evidence for the Contributive Role of the Right Inferior Fronto-Occipital Fasciculus in Non-Verbal Semantic Cognition.” *Brain Structure & Function* 222 (4): 1597–610. https://doi.org/10.1007/s00429-016-1294-x.

Herbet, Guillaume, Ilyess Zemmoura, and Hugues Duffau. 2018. “Functional Anatomy of the Inferior Longitudinal Fasciculus: From Historical Reports to Current Hypotheses.” *Frontiers in Neuroanatomy* 12. https://doi.org/10.3389/fnana.2018.00077.

Horowitz-Kraus, Tzipi, Yingying Wang, Elena Plante, and Scott K. Holland. 2014. “Involvement of the Right Hemisphere in Reading Comprehension: A DTI Study.” *Brain Research* 1582 (September): 34–44. https://doi.org/10.1016/j.brainres.2014.05.034.

Hua, Kegang, Jiangyang Zhang, Setsu Wakana, et al. 2008. “Tract Probability Maps in Stereotaxic Spaces: Analyses of White Matter Anatomy and Tract-Specific Quantification.” *NeuroImage* 39 (1): 336–47. https://doi.org/10.1016/j.neuroimage.2007.07.053.

Hughlings Jackson, John. 1874. “On the Nature of the Duality of the Brain.” *Medical Press and Circular* 1: 80–86.

Hughlings Jackson, John. 1879. “On Affections of Speech from Disease of the Brain.” *Brain* 2 (2): 203–22. https://doi.org/10.1093/brain/2.2.203.

Ivanova, Maria V., Dmitry Yu. Isaev, Olga V. Dragoy, et al. 2016. “Diffusion-Tensor Imaging of Major White Matter Tracts and Their Role in Language Processing in Aphasia.” *Cortex* 85 (December): 165–81. https://doi.org/10.1016/j.cortex.2016.04.019.

Ivanova, Maria V., Allison Zhong, And Turken, Juliana V. Baldo, and Nina F. Dronkers. 2021. “Functional Contributions of the Arcuate Fasciculus to Language Processing.” *Frontiers in Human Neuroscience* 15: 672665. https://doi.org/10.3389/fnhum.2021.672665.

Kargar, Yasin, and Milad Jalilian. 2024. “Anatomo-Functional Profile of White Matter Tracts in Relevance to Language: A Systematic Review.” *Journal of Neurolinguistics* 69 (February): 101175. https://doi.org/10.1016/j.jneuroling.2023.101175.

Kemerdere, Rahsan, Nicolas Menjot de Champfleur, Jérémy Deverdun, et al. 2016. “Role of the Left Frontal Aslant Tract in Stuttering: A Brain Stimulation and Tractographic Study.” *Journal of Neurology* 263 (1): 157–67. https://doi.org/10.1007/s00415-015-7949-3.

Kinoshita, Masashi, Nicolas Menjot de Champfleur, Jeremy Deverdun, Sylvie Moritz-Gasser, Guillaume Herbet, and Hugues Duffau. 2015. “Role of Fronto-Striatal Tract and Frontal Aslant Tract in Movement and Speech: An Axonal Mapping Study.” *Brain Structure & Function* 220 (6): 3399–412. https://doi.org/10.1007/s00429-014-0863-0.

Kourtidou, Evie, Dimitrios Kasselimis, Georgia Angelopoulou, et al. 2021. “The Role of the Right Hemisphere White Matter Tracts in Chronic Aphasic Patients After Damage of the Language Tracts in the Left Hemisphere.” *Frontiers in Human Neuroscience* 15 (June). https://doi.org/10.3389/fnhum.2021.635750.

Landers, Maud J. F., Stephan P. L. Meesters, Martine van Zandvoort, Wouter de Baene, and Geert-Jan M. Rutten. 2022. “The Frontal Aslant Tract and Its Role in Executive Functions: A Quantitative Tractography Study in Glioma Patients.” *Brain Imaging and Behavior* 16 (3): 1026–39. https://doi.org/10.1007/s11682-021-00581-x.

Lanser, J. B. K., W. H. C. Van Santen, A. Jennekens-Schinkel, and R. a. C. Roos. 1993. “Tourette’s Syndrome and Right Hemisphere Dysfunction.” *The British Journal of Psychiatry* 163 (1): 116–18. https://doi.org/10.1192/bjp.163.1.116.

Latini, Francesco, Johanna Mårtensson, Elna Marie Larsson, et al. 2017. “Segmentation of the Inferior Longitudinal Fasciculus in the Human Brain: A White Matter Dissection and Diffusion Tensor Tractography Study.” *Brain Research* 1675: 102–15. https://doi.org/10.1016/j.brainres.2017.09.005.

Li, Yijie, Wei Zhang, Ye Wu, et al. 2024. “A Diffusion MRI Tractography Atlas for Concurrent White Matter Mapping across Eastern and Western Populations.” *Scientific Data* 11 (July): 787. https://doi.org/10.1038/s41597-024-03624-2.

López-Barroso, Diana, Marco Catani, Pablo Ripollés, Flavio Dell’Acqua, Antoni Rodríguez-Fornells, and Ruth de Diego-Balaguer. 2013. “Word Learning Is Mediated by the Left Arcuate Fasciculus.” *Proceedings of the National Academy of Sciences* 110 (32): 13168–73. https://doi.org/10.1073/pnas.1301696110.

Maffei, C., C. Lee, M. Planich, et al. 2021. “Using Diffusion MRI Data Acquired with Ultra-High Gradient Strength to Improve Tractography in Routine-Quality Data.” *NeuroImage* 245 (December): 118706. https://doi.org/10.1016/j.neuroimage.2021.118706.

Mandonnet, Emmanuel, Peter A. Winkler, and Hugues Duffau. 2010. “Direct Electrical Stimulation as an Input Gate into Brain Functional Networks: Principles, Advantages and Limitations.” *Acta Neurochirurgica* 152 (2): 185–93. https://doi.org/10.1007/s00701-009-0469-0.

Mitchell, Rachel L. C., and Tim J. Crow. 2005. “Right Hemisphere Language Functions and Schizophrenia: The Forgotten Hemisphere?” *Brain: A Journal of Neurology* 128 (Pt 5): 963–78. https://doi.org/10.1093/brain/awh466.

Mori, S, S Wakana, L.M. Nagae-Poetscher, and P.C.M. van Zijl. 2005. *MRI Atlas of Human White Matter*. Elsevier. https://shop.elsevier.com/books/mri-atlas-of-human-white-matter/mori/978-0-444-51741-8.

Mori, Susumu, Kenichi Oishi, Hangyi Jiang, et al. 2008. “Stereotaxic White Matter Atlas Based on Diffusion Tensor Imaging in an ICBM Template.” *NeuroImage* 40 (2): 570–82. https://doi.org/10.1016/j.neuroimage.2007.12.035.

Moritz-Gasser, Sylvie, Guillaume Herbet, and Hugues Duffau. 2013. “Mapping the Connectivity Underlying Multimodal (Verbal and Non-Verbal) Semantic Processing: A Brain Electrostimulation Study.” *Neuropsychologia* 51 (10): 1814–22. https://doi.org/10.1016/j.neuropsychologia.2013.06.007.

Neef, Nicole E, Alfred Anwander, Christoph Bütfering, et al. 2018. “Structural Connectivity of Right Frontal Hyperactive Areas Scales with Stuttering Severity.” *Brain* 141 (1): 191–204. https://doi.org/10.1093/brain/awx316.

Ng, Sam, Sylvie Moritz-Gasser, Anne-Laure Lemaitre, Hugues Duffau, and Guillaume Herbet. 2021. “White Matter Disconnectivity Fingerprints Causally Linked to Dissociated Forms of Alexia.” *Communications Biology* 4 (1): 1413. https://doi.org/10.1038/s42003-021-02943-z.

O’Donnell, Lauren J., Yannick Suter, Laura Rigolo, et al. 2017. “Automated White Matter Fiber Tract Identification in Patients with Brain Tumors.” *NeuroImage: Clinical* 13 (January): 138–53. https://doi.org/10.1016/j.nicl.2016.11.023.

O’Donnell, Lauren J., and Carl-Fredrik Westin. 2007. “Automatic Tractography Segmentation Using a High-Dimensional White Matter Atlas.” *IEEE Transactions on Medical Imaging* 26 (11): 1562–75. https://doi.org/10.1109/TMI.2007.906785.

Oldfield, R. C. 1971. “The Assessment and Analysis of Handedness: The Edinburgh Inventory.” *Neuropsychologia* 9 (1): 97–113. https://doi.org/10.1016/0028-3932(71)90067-4.

Olivé, Guillem, Claudia Peñaloza, Lucía Vaquero, Matti Laine, Nadine Martin, and Antoni Rodriguez-Fornells. 2023. “The Right Uncinate Fasciculus Supports Verbal Short-Term Memory in Aphasia.” *Brain Structure & Function* 228 (3–4): 875–93. https://doi.org/10.1007/s00429-023-02628-9.

Pacella, Valentina, Michele Scandola, Maddalena Beccherle, et al. 2020. “Anosognosia for Theory of Mind Deficits: A Single Case Study and a Review of the Literature.” *Neuropsychologia* 148 (November): 107641. https://doi.org/10.1016/j.neuropsychologia.2020.107641.

Paldino, M.J., K. Hedges, and F. Golriz. 2016. “The Arcuate Fasciculus and Language Development in a Cohort of Pediatric Patients with Malformations of Cortical Development.” *AJNR: American Journal of Neuroradiology* 37 (1): 169–75. https://doi.org/10.3174/ajnr.A4461.

Pani, Ethan, Xin Zheng, Jasmine Wang, Andrea Norton, and Gottfried Schlaug. 2016. “Right Hemisphere Structures Predict Poststroke Speech Fluency.” *Neurology* 86 (17): 1574–81. https://doi.org/10.1212/WNL.0000000000002613.

Papagno, Costanza, Alessandra Casarotti, Alessandro Comi, et al. 2016. “Long-Term Proper Name Anomia after Removal of the Uncinate Fasciculus.” *Brain Structure & Function* 221 (1): 687–94. https://doi.org/10.1007/s00429-014-0920-8.

Papagno, Costanza, Christiano Miracapillo, Alessandra Casarotti, et al. 2011. “What Is the Role of the Uncinate Fasciculus? Surgical Removal and Proper Name Retrieval.” *Brain* 134 (2): 405–14. https://doi.org/10.1093/brain/awq283.

Price, Cathy J., and Karl J. Friston. 2002. “Degeneracy and Cognitive Anatomy.” *Trends in Cognitive Sciences* 6 (10): 416–21. https://doi.org/10.1016/s1364-6613(02)01976-9.

Radwan, Ahmed M., Stefan Sunaert, Kurt Schilling, et al. 2022. “An Atlas of White Matter Anatomy, Its Variability, and Reproducibility Based on Constrained Spherical Deconvolution of Diffusion MRI.” *NeuroImage* 254 (July): 119029. https://doi.org/10.1016/j.neuroimage.2022.119029.

Riès, Stéphanie K., Nina F. Dronkers, and Robert T. Knight. 2016. “Choosing Words: Left Hemisphere, Right Hemisphere, or Both? Perspective on the Lateralization of Word Retrieval.” *Annals of the New York Academy of Sciences* 1369 (1): 111–31. https://doi.org/10.1111/nyas.12993.

Rojkova, K., E. Volle, M. Urbanski, F. Humbert, F. Dell’Acqua, and M. Thiebaut de Schotten. 2016. “Atlasing the Frontal Lobe Connections and Their Variability Due to Age and Education: A Spherical Deconvolution Tractography Study.” *Brain Structure & Function* 221 (3): 1751–66. https://doi.org/10.1007/s00429-015-1001-3.

Román, Claudio, Miguel Guevara, Ronald Valenzuela, et al. 2017. “Clustering of Whole-Brain White Matter Short Association Bundles Using HARDI Data.” *Frontiers in Neuroinformatics* 11 (December). https://doi.org/10.3389/fninf.2017.00073.

Román, Claudio, Cecilia Hernández, Miguel Figueroa, et al. 2022. “Superficial White Matter Bundle Atlas Based on Hierarchical Fiber Clustering over Probabilistic Tractography Data.” *NeuroImage* 262 (November): 119550. https://doi.org/10.1016/j.neuroimage.2022.119550.

Ros, Christian, Daniel Güllmar, Martin Stenzel, Hans-Joachim Mentzel, and Jürgen Rainer Reichenbach. 2013. “Atlas-Guided Cluster Analysis of Large Tractography Datasets.” *PLOS ONE* 8 (12): e83847. https://doi.org/10.1371/journal.pone.0083847.

Schlaug, Gottfried, Sarah Marchina, and Andrea Norton. 2008. “From Singing to Speaking: Why Singing May Lead to Recovery of Expressive Language Function in Patients with Broca’s Aphasia.” *Music Perception* 25 (4): 315–23. https://doi.org/10.1525/MP.2008.25.4.315.

Sheppard, Shannon M., Lynsey M. Keator, Bonnie L. Breining, et al. 2020. “Right Hemisphere Ventral Stream for Emotional Prosody Identification: Evidence from Acute Stroke.” *Neurology* 94 (10): e1013–20. https://doi.org/10.1212/WNL.0000000000008870.

Shu, Ni, Yaou Liu, Yunyun Duan, and Kuncheng Li. 2015. “Hemispheric Asymmetry of Human Brain Anatomical Network Revealed by Diffusion Tensor Tractography.” *BioMed Research International* 2015. https://doi.org/10.1155/2015/908917.

Suarez, Ralph O., Olivier Commowick, Sanjay P. Prabhu, and Simon K. Warfield. 2012. “Automated Delineation of White Matter Fiber Tracts with a Multiple Region-of-Interest Approach.” *Neuroimage* 59 (4): 3690–700. https://doi.org/10.1016/j.neuroimage.2011.11.043.

Tang, Yuchun, Wei Sun, Arthur W. Toga, John M. Ringman, and Yonggang Shi. 2018. “A Probabilistic Atlas of Human Brainstem Pathways Based on Connectome Imaging Data.” *NeuroImage* 169 (April): 227–39. https://doi.org/10.1016/j.neuroimage.2017.12.042.

Thiebaut de Schotten, Michel, Laurent Cohen, Eduardo Amemiya, Lucia W. Braga, and Stanislas Dehaene. 2014. “Learning to Read Improves the Structure of the Arcuate Fasciculus.” *Cerebral Cortex (New York, N.Y.: 1991)* 24 (4): 989–95. https://doi.org/10.1093/cercor/bhs383.

Thiebaut de Schotten, Michel, Dominic H. Ffytche, Alberto Bizzi, et al. 2011. “Atlasing Location, Asymmetry and Inter-Subject Variability of White Matter Tracts in the Human Brain with MR Diffusion Tractography.” *NeuroImage* 54 (1): 49–59. https://doi.org/10.1016/j.neuroimage.2010.07.055.

Thiebaut de Schotten, Michel, Chris Foulon, and Parashkev Nachev. 2020. “Brain Disconnections Link Structural Connectivity with Function and Behaviour.” *Nature Communications*, ahead of print. https://doi.org/10.1038/s41467-020-18920-9.

Vallesi, Antonino, and Laura Babcock. 2020. “Asymmetry of the Frontal Aslant Tract Is Associated with Lexical Decision.” *Brain Structure and Function* 225 (3): 1009–17. https://doi.org/10.1007/s00429-020-02054-1.

Vassal, François, Claire Boutet, Jean-Jacques Lemaire, and Christophe Nuti. 2014. “New Insights into the Functional Significance of the Frontal Aslant Tract: An Anatomo-Functional Study Using Intraoperative Electrical Stimulations Combined with Diffusion Tensor Imaging-Based Fiber

Tracking." *British Journal of Neurosurgery* 28 (5): 685–87. https://doi.org/10.3109/02688697.2014.889810.

Von Der Heide, Rebecca J., Laura M. Skipper, Elizabeth Klobusicky, and Ingrid R. Olson. 2013. "Dissecting the Uncinate Fasciculus: Disorders, Controversies and a Hypothesis." *Brain* 136 (6): 1692–707. https://doi.org/10.1093/brain/awt094.

Wakana, Setsu, Arvind Caprihan, Martina M. Panzenboeck, et al. 2007. "Reproducibility of Quantitative Tractography Methods Applied to Cerebral White Matter." *NeuroImage* 36 (3): 630–44. https://doi.org/10.1016/j.neuroimage.2007.02.049.

Wu, Yupeng, Dandan Sun, Yong Wang, and Yibao Wang. 2016. "Subcomponents and Connectivity of the Inferior Fronto-Occipital Fasciculus Revealed by Diffusion Spectrum Imaging Fiber Tracking." *Frontiers in Neuroanatomy* 10 (SEP). https://doi.org/10.3389/fnana.2016.00088.

Yang, Chengmin, Li Yao, Naici Liu, et al. 2021. "Microstructural Abnormalities of White Matter Across Tourette Syndrome: A Voxel-Based Meta-Analysis of Fractional Anisotropy." *Frontiers in Neurology* 12 (September). https://doi.org/10.3389/fneur.2021.659250.

Yeh, Fang-Cheng, Sandip Panesar, David Fernandes, et al. 2018. "Population-Averaged Atlas of the Macroscale Human Structural Connectome and Its Network Topology." *NeuroImage* 178 (September): 57–68. https://doi.org/10.1016/j.neuroimage.2018.05.027.

Yendiki, Anastasia, Patricia Panneck, Priti Srinivasan, et al. 2011. "Automated Probabilistic Reconstruction of White-Matter Pathways in Health and Disease Using an Atlas of the Underlying Anatomy." *Frontiers in Neuroinformatics* 5 (October): 23. https://doi.org/10.3389/fninf.2011.00023.

Yoo, Sang Wook, Pamela Guevara, Yong Jeong, et al. 2015. "An Example-Based Multi-Atlas Approach to Automatic Labeling of White Matter Tracts." *PLOS ONE* 10 (7): e0133337. https://doi.org/10.1371/journal.pone.0133337.

Zhang, Fan, Ye Wu, Isaiah Norton, et al. 2018. "An Anatomically Curated Fiber Clustering White Matter Atlas for Consistent White Matter Tract Parcellation across the Lifespan." *NeuroImage* 179 (October): 429–47. https://doi.org/10.1016/j.neuroimage.2018.06.027.